UiT The Arctic University of Norway

Faculty of Science and Technology
Department of Geosciences

Superimposed macro- and mesoscale folds, and their relation to ductile shear zones in the Karasjok Greenstone Belt, Finnmark, Norway

Eirik Bache Stokmo

Master's thesis in Geology Geo-3900 June 2020

Abstract

The Karasjok Greenstone Belt (KGB) is a N-S trending supracrustal belt in Northern Norway. The KGB may comprise economically important mineral resources. Thus, a better understanding of ore genesis and structural architecture is key information for future exploration. The purpose of this master thesis is to perform detailed structural analysis based on field work in the northern part of KGB. Field data will be combined with exsiting geological data and integrated with high-resolution ortho-photos and aeromagnetic data from Lakselv. This will be used as a basis for interpreting the structural architecture in more detail and to compare it with other areas of the KGB.

The present work shows that the stratigraphic sequence is partly inverted. This is likely due to macro-scale overturned folding and possible imbrication. A detailed study of F1 and F2 folds show Ramsey type 2 interference fold patterns. The type 2 pattern suggests NW directed folding and imbricate shearing which is partly in contrast with previous D1 deformation models. The D1 deformation event is followed by strongly asymmetric SW vergent D2 shear folding. Finally, small scale ductile D3 shear zones produced moderately plunging drag folds and fault-propagation folds. The D1 and D3 events in the Lakselv area are not evident farther south in the KGB. Here, the magnetic data mostly show linear NW-SE striking anomalies. This might correspond to D2 structural trends seen in Lakselv. The southernmost part of the KGB shows an anomaly pattern that resembles the refolded pattern in Lakselv.

The proposed new D1 model with imbricate folding and associated local inversion may correspond with structures in the northeastern parts of the Kautokeino Greenstone Belt, the Repparfjorden Tectonic Window, and magnetic anomalies within the Jergul Gneiss Complex. The relative timing of the deformation as well as the tectonic evolution correspond with both Svecofennian- and Lapland-Kola deformation. Further work is needed to confirm that the D1 phase within the study area is not a local anomaly and also constrain the deformation event in time.

Acknowledgments

Firstly I would like to thank my supervisors; Harald Hansen(UiT) for allowing me to tag along on multiple field-trips and continued support throughout the process of writing this thesis, I hope it hasn't affected your work. Steffen Bergh (UiT) for your incredible enthusiasm and knowledge of geology, I am grateful for the help throughout my stay at the University of Tromsø. Kerstin Saalmann (NGU) for the help in the field and interesting discussions, thank you. Also I would like to thank my family for continued support. Finally, I would like to thank my field-assistant, partner and fellow Ingvild Brynjulvsrud Bakke for being patient during the four weeks living in a tent with me at Lakselv, and then had to convert our apartment into an office during the Covid-19 lockdown.

Contents

List of Figures

Chapter 1

Introduction

1.1 Preface

The thesis is part of an ongoing project at the Department of Geosciences at UiT-The Arctic University of Norway (UiT), entitled "Tectono-magmatic evolution of Archean-Palaeoproterozoic volcanic and sedimentary rocks (greenstone belts) in northern Norway". The main project, which is in collaboration with Geological Survey of Norway (NGU), has an interdisciplinary aim to provide knowledge about greenstone belts structure, age, petrology, geochemistry, metamorphic conditions, ore/mineral resource potential, and tectono-magmatic evolution (Corfu et al., 2003; Bergh et al., 2010, 2015; Myhre et al., 2011, 2013). This thesis is part of a UiT-NGU field-oriented research campaign focusing on volcanic and sedimentary rocks of the Karasjok Greenstone Belt (KGB) near Lakselv, Finnmark, aiming to study in more detail polyphase fold and thrust structures in the supracrustal units.

1.2 Context of the study

The northern Fennoscandian Shield (Figs.1.1, 1.2 and 1.3) hosts numerous Archean to Palaeoproterozoic greenstone belts that are often intensively orogenic deformed, structurally complex and rich in metals. In Northern Norway, the greenstone belts occur both in tectonic windows within the Caledonian thrust nappes as well as west and south east of the Caledonides (Fig.1.2). They are mostly surrounded by Neoarchean TTG-gneisses and younger ca 1.8 Ga magmatic rocks. New airborne geophysical data (Gravity/FTG and Magnetic surveys) were obtained by NGU's governmental funded program "Mineral resources in Norther Norway" (MINN) in the period 2011-2014. This data help to unravel the regional structural architecture and complex deformation related to crustal scale ductile shear zones. The data also confirm a direct correlation of orogenic related greenstone belts west of, and

inside the Scandinavian Caledonides, with those in Finland and Northern Sweden (Bergmann, 2018).

Recent geochronological work by Hansen et al. (2020) revealed the large time-span between deposition of the supracrustal rocks withing the Karasjok Greenstone Belt (2.7–1.95 Ga). This time frame could therefore imply that some parts of the belt have experienced up to three orogneies. This work is focusing on how Archean to Palaeoproterozoic supracrustal rocks (greenstone belts) were deformed during the Lapland-Kola orogeny and the possible later or earlier effects of the Svecofennian orogeny. And, how polyphase crustal deformation affects the resulting architecture.

Deformation of an ore body can alter its potential for extraction as well as promote the formation of new environments for ore forming processes (Eilu et al., 2003; Saalmann et al., 2010; Saalmann and Niiranen, 2010; Eilu and Ojala, 2011; Saalmann and Laine, 2014; Eilu, 2017; Groves et al., 2018). Also, new high resolution geophysical data (Sandstad, 2015; Nasuti et al., 2015) provide additional information about more deep seated ore bodies. A combination of the geophysical data with structural field data presented in this paper could help mineral exploration.

1.3 Purpose of the study

The aim of this thesis is to investigate the structural architecture of the northern-most part of the Karasjok Greenstone Belt (KGB). This study is mostly based on fieldwork and aims to determine if the KGB went through several tectonic events or if the deformation can be explained by one complex progressive orogenic event. The study also investigates if the deformation is typical for a modern type orogeny. Finally, this work aims to correlate the northern KGB with other similar terrains in Fennoscandia. For instance, were the Karasjok- and Kautokeino Greenstone belts part of the same basin and/or share similar deformation? Is it possible to infer structural information based on geophysical data in less exposed areas of the KGB?

1.4 Geological Setting

1.4.1 The Fennoscandian Shield

The Fennoscandian Shield (also known as the Baltic Shield) is the north-eastern part of the East European Craton and consists of several crustal segments (Fig.1.1). The Fennoscandian Shield was formed during multiple orogenic/accretionary events from Archean to early Mesoproterozoic (3.5–1.5 Ga). The cryptic Saamian orogeny (3.1–2.9 Ga) formed a belt of high-grade gneisses dominantly of tonalitic-trondhjemitic-granodioritic composition which form the basement of the Archean greenstone belts

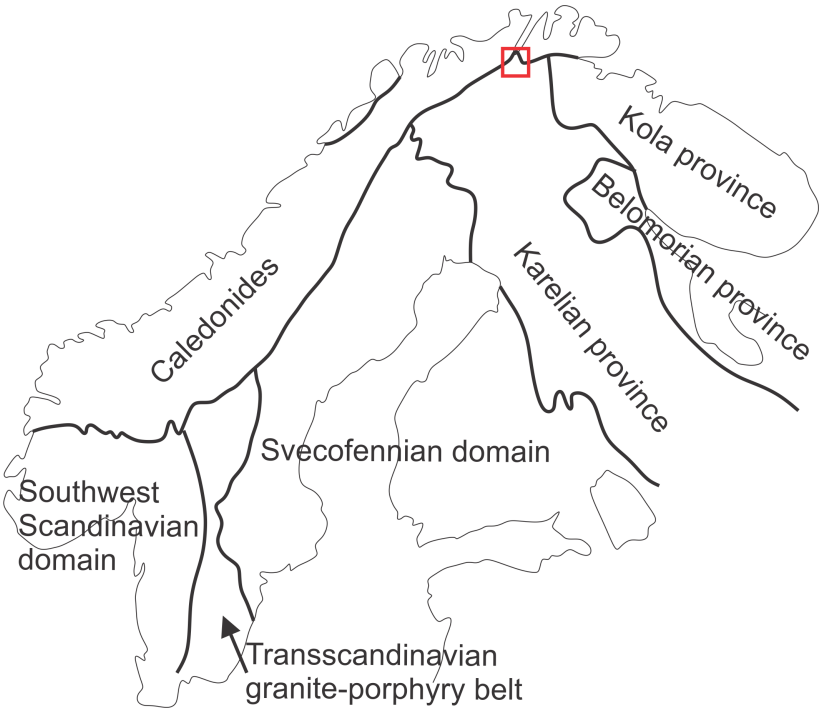

Figure 1.1: Crustal segments of the Fennoscandian shield (Lahtinen et al., 2005). Study area marked with red square.

(Gaál and Gorbatschev, 1987). The Lopian orogeny (2.9–2.6 Ga) large volumes of crust was generated both as supracrustals and as tonalitic to trondhjemitic intrusions. A major rifting event at 2.5–2.0 Ga produced a large number of volcano-sedimentary basins (Gorbatschev and Bogdanova, 1993). During the Lapland-Kola orogeny (1.95–1.79 Ga) the Kola Ocean started to close gradually, deforming and closed the basins forming orogenic scale belts(Lahtinen and Huhma, 2019) and during the subsequent, composite, Svecofennian orogeny (1.92–1.79 Ga) (Lahtinen et al., 2005, 2008) final closure of the rift basins occurred by continent-continent collision. These orogenic events led to a very complex system of mixed rift-related and accretionary basins filled by volcano-sedimentary successions (greenstone belts) like in the KGB. To the southwest the Svecofennian domain is truncated by the N-S trending Transscandinavian Ignous Belt (1.8–1.65) (Gorbatschev and Bogdanova, 1993). The Southwest Scandinavian domain consist of rocks reworked during several tectonic events; Gothian, Sveconorwegian, Grenvillian orogenies (1.75–0.9 Ga) (Gaál and Gorbatschev, 1987).

1.4.2 The Karasjok Greenstone Belt

The Karasjok Greenstone Belt (KGB) is a N-S trending metasupracrustal belt in the Eastern parts of the Finnmark plateau (Fig.1.3). It can be traced southwards through Finland and in to Russia.The Caledonian Nappes overlie the greenstone

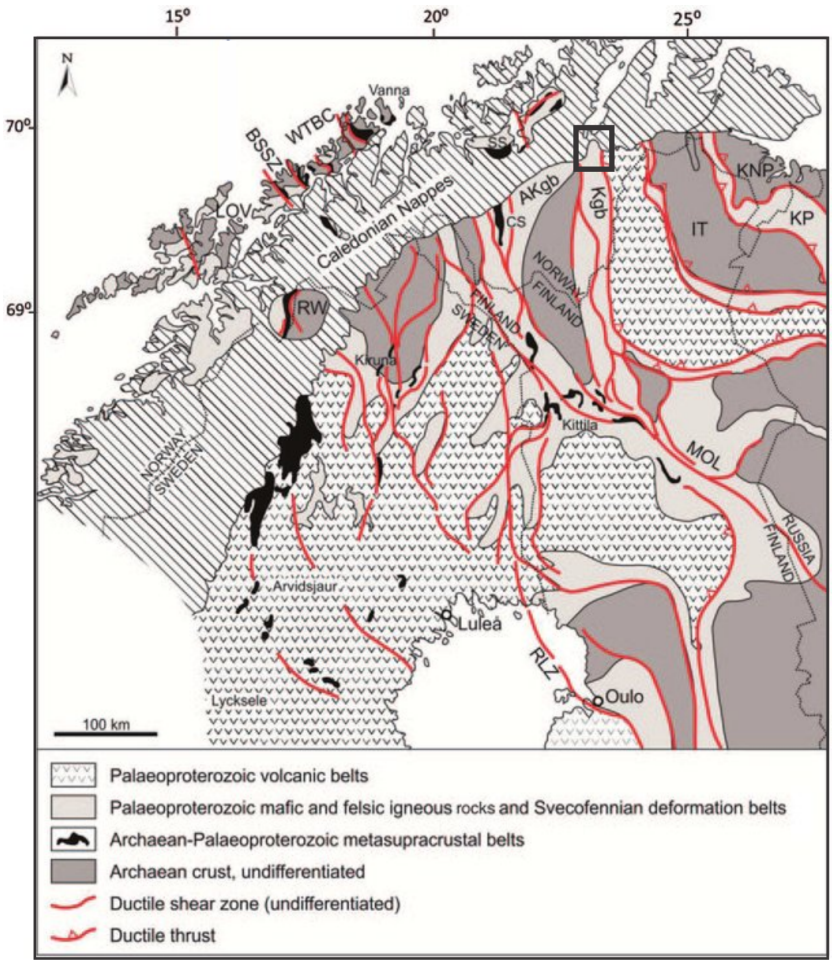

Figure 1.2: Regional structural map of northern Fennoscandia showing Archean and Palaeoproterozoic crust and the basement outliers within and to the west of the Scandinavian Caledonides. Note correlation of basement regions below the Caledonides, including supracrustal belts, magmatic rocks, and network of ductile shear terrane boundaries?. Black frame locates the study area. The map is modified from Marker (1985); Gaál and Gorbatschev (1987); Gorbatschev and Bogdanova (1993); Karki et al. (1993); Hanski et al. (2001); Bergh et al. (2007)

belt in the north. The KGB is sandwiched between the 3.0–2.7 Ga TTG dominated Jergul Complex (Bingen et al., 2016; Hansen et al., 2020) in the west, and the Tanaelv Migmatite Belt (TMB) to the east. The contact between KGB and the Jergul Complex is inferred as a possible thrust or at least an unconformably overlying the Jergul Complex (Siedlecka et al., 1985). A west-vergent thrust marks the boundary between the KGB and the TMB (Krill, 1985; Braathen and Davidsen, 2000). The Levajok Granulite Complex (LGC) is thrusted on top of the TMB. The LGC consists of granulite facies metasedimentary and mafic to intermediate igneous rocks (Krill, 1985; Gaál and Gorbatschev, 1987). The age of the Levajok Granulite Complex is not known, but the metamorphism and igneous activity are thought to have happened c.2.0–1.9 Ga ago (Krill et al., 1985). The TMB consists of a high- to medium-grade sequence of partly migmatitic rocks and is bound by a mylonitic

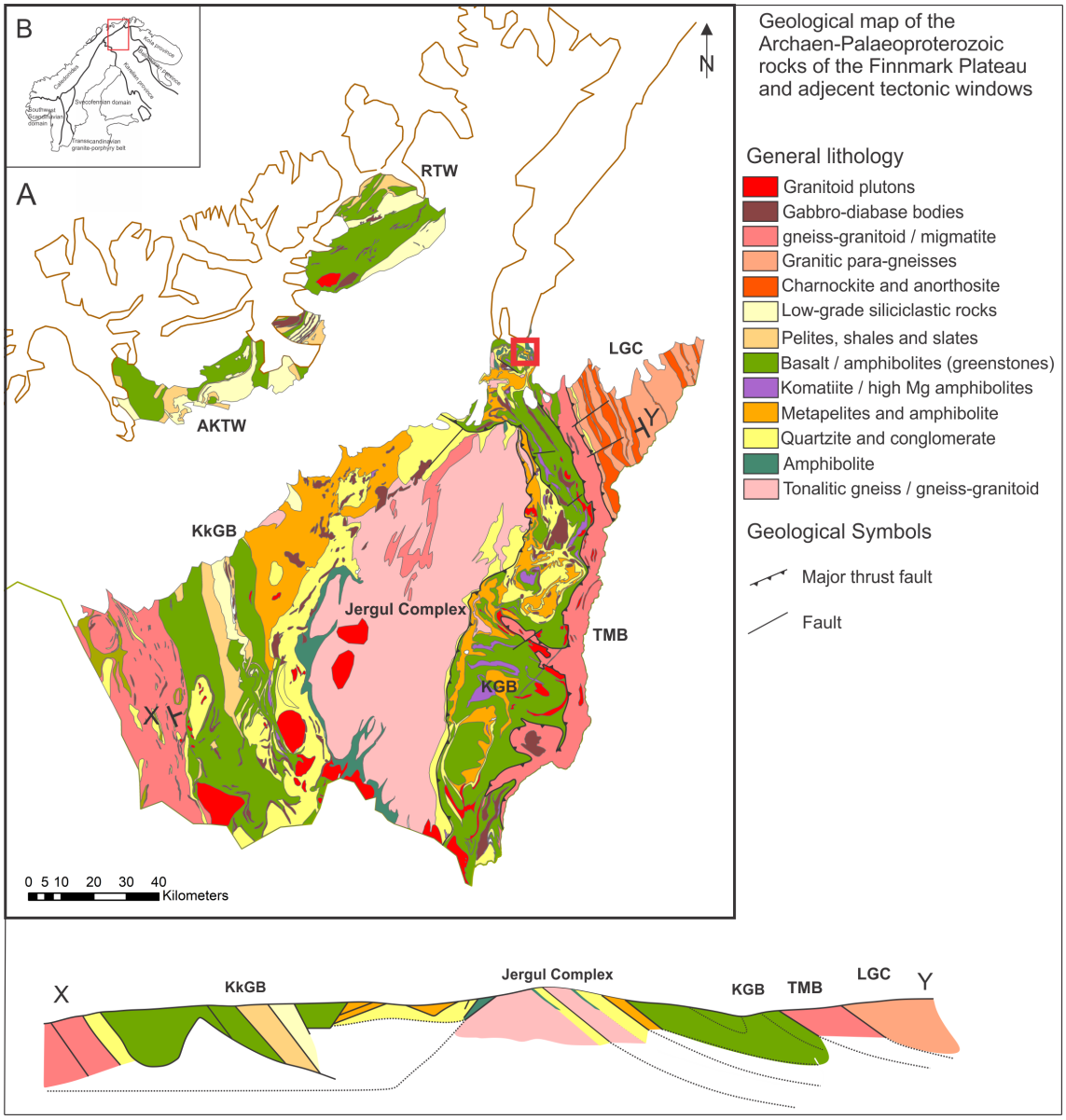

Figure 1.3: A: Simplified geological map of the Archean and Palaeoproterozoic rocks of the Finnmark Plateau, red square showing the study area, modified from (Olesen and Sandstad, 1993; Siedlecka et al., 1985; Torgersen et al., 2015; Bingen et al., 2016). B: location of map A relative to the Fennoscandian shield (Lahtinen et al., 2005). Schematic profile SW-NE based on gravimetric and structural data from the Kautokeino Greenstone Belt (Olesen and Sandstad, 1993; Henderson et al., 2016) and structural data from the KGB, TMB and LC (Krill, 1985; Often, 1985; Braathen and Davidsen, 2000). Abbreviations:AKTW Alta Kvænangen Tectonic Window, RWT Repparfjord Tectonic Window, LGC Levajok Granulite Complex, TMB Tanaelv Migmatite Belt, KGB Karasjok Greenstone Belt, KkGB Keutokeino Greenstone Belt

shear zone towards KGB (Braathen and Davidsen, 2000). The age is thought to be similar to the Levajok Granulite Complex and formed during a westward thrusting of the Levajok Granulite Complex during the Lapland-Kola orogeny (Gaál and Gorbatschev, 1987; Braathen and Davidsen, 2000). The time of deposition of the rocks within the KGB remains poorly dated, however recent work by Melezhik et al. (2015) and Hansen et al. (2020) suggest an Archean (3.0–2.2 Ga) basement overlain by two separate Archean (2.7 Ga) and Palaeoproterozic (2.2–1.95 Ga) supracrustal sequences.

1.4.3 Stratigraphy and sedimentary formations of the KGB

Several stratigraphic sequences have been suggested for different parts of the KGB (Siedlecka et al., 1985; Often, 1985; Davidsen, 1994; Braathen and Davidsen, 2000). For simplicity the names used in this thesis will be derived from work in the northern parts of the KGB (Davidsen, 1994; Braathen and Davidsen, 2000). Formation names used in other parts of the KGB (Siedlecka et al., 1985; Often, 1985) will be in brackets next to the most likely correlatable formation from the northern parts. Efforts of correlating units have been tried by several authors and a compilation of the different stratigraphies are shown in figure 1.4 together with geochronological data.

The Lavttevárri Formation (Voumegielas Formation) The 50–150 m thick Lavttevárri formation constitutes a small part of the KGB north of the Jergul Complex (Fig.1.3), as well as larger areas near the town of Lakselv (Fig.1.5). It is the lowermost unit of the KGB (Siedlecka et al., 1985; Often, 1985; Davidsen, 1994; Braathen and Davidsen, 2000). The formation consists mainly of foliated amphibolite, but some biotite-rich argillitic layers occur together with komatiites (Siedlecka et al., 1985; Braathen and Davidsen, 2000). In the Lakselv area a "leptite" occurs which is interpreted to be a rhyllitic extrusive (Davidsen, 1994) Siedlecka et al. (1985) correlated this formation with the 2781 ± 4 Ma old Gål'denvarri formation in the Kautokeino Greenstone Belt (Bingen, et al., 2015). Recent dating of a ultramafic intrusive within the Lavttevárri Formation in the Lakselv area showed an age of 2721 ± 11 Ma (Hansen et al., 2020). The contact with the basal gneisses is somewhat diffuse and shows both conformable contacts (Davidsen, 1994) as well as angular unconformity (Andreassen, 1993) and possible thrust contacts (Siedlecka et al., 1985) depending on the area.

The Čorgaš Formation (Skuvvanvarri Formation and Gollebáiki Formation) The 250–700 m thick Čorgaš Formation is most prominent in the Lakselv area, in central parts of the belt and along the contact to the Jergul Complex along

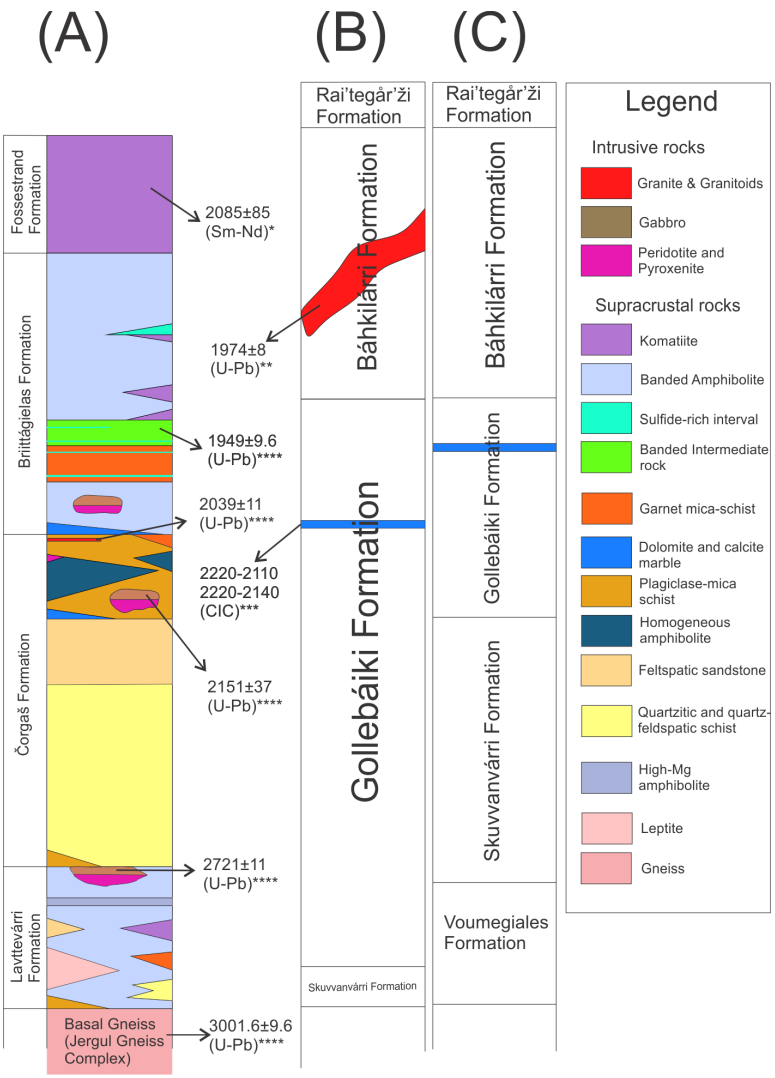

Figure 1.4: Correlation of stratigraphy. A:(Hansen et al., 2020) (modified from Davidsen (1994)). B and C: (Often, 1985). Geochronology data: (*) - Krill et al. (1985), (**) - Marker et al. (2000), (***) - Melezhik et al. (2015), (****) - Hansen et al. (2020). Entire figure modifed from Melezhik et al. (2015)

the western boundary (Fig.1.3). It consists mostly of sedimentary rocks as conglomerates, sandstone, mudstone and carbonate sequences (Siedlecka et al., 1985; Davidsen, 1994; Melezhik et al., 2015). In some places, fuchsite bearing quartzite and conglomerate occur. In addition, homogenous amphibolites and layered intrusions are prominent within the Čorgaš Formation. The lower boundary to the Lavttevárri Formation is not consistent and in parts of the belt the Čorgaš Formation lies conformably on the Jer'Gul Gneiss Complex (Often, 1985). In other areas the contact is an angular unconformity (Siedlecka et al., 1985) or is described as sharp (Davidsen, 1994). According to Siedlecka et al. (1985); Braathen and Davidsen (2000) the upper boundary with the Briittagielás is marked by a thrust fault, which shows a similar westward thrusting direction as the Tanaelv Migmatite Complex. In the Lakselv area these large thrusts have not been identified, however, small

shear zones and minor foliation parallel dip-slip thrusts have been identified within the Čorgaš Formation (this paper). The absolute age of the Čorgaš Formation is not known. Siedlecka et al 1985, correlated the Skuvvanvarri Formation (Čorgaš) with the Masi Formation in Kautokeino, which has a minimum age of 2220 ± 7 Ma (Bingen et al., 2016). New U-Pb dating of a gabbroic intrusive near the contact with the Lavttevárri Formation indicates a maximum age of 2721 ± 11 Ma for the Čorgaš Formation (Hansen et al., 2020). Furthermore, a mafic intrusive at the upper level of the formation yielded an age of 2151 ± 37 (Hansen et al., 2020) which constrain the formation to a 2700-2150 Ma interval. Previous carbon isotope chemostratigraphy dating on calcite and dolomite marbles indicate a depositional age between 2220 and 2140 Ma (Melezhik et al., 2015).

The Briittágielas Formation (Báhkilvárri Formation) The 300–700 m thick Briittágielas Formation is dominated by banded amphibolites. Garnet mica schist ,a banded intermediate volcanite and several sulfide- and metakomatiitic horizons are interclated within the formation (Davidsen, 1994). The intermediate volcanic unit has been dated to 1949 ± 9 Ma (Hansen et al., 2020).

The Fossestrand Formation The more than 300 m thick Fossestrand Formation consists mostly of metakomatiitc rocks with pillow structures and volcaniclastic material (Davidsen, 1994). It appears in the core of regional-scale, isoclinal folds (Braathen and Davidsen, 2000). Some course-grained gabbroic bodies are found within the formation accompanied with minor metaperidotites (Davidsen, 1994)

Paleo-tectonic setting In the northern areas, no tectonic breaks have been identified and therefore assumed to be a lithostratigraphy. The paleo-tectonic setting for the Lakselv area is interpreted to be intra continental, based on the contact with the underlying basement and the negative Nd anomalies in the tholeiitic metabasites. Deposited under sub-aquatic conditions based on the occurence of pillow lavas and graphite bearing schists (Davidsen, 1994; Braathen and Davidsen, 2000).

1.4.4 Structural and metamorphic overview of the Karasjok Greenstone Belt

Three ductile deformational phases have been identified in the KGB (Pharaoh, 1981; Nilsen, 1988, 1989; Braathen, 1991; Andreassen, 1993; Davidsen, 1994; Braathen and Davidsen, 2000). Based on overprinting relationships the relative age of each event/phase has also been identified. Previous authors therefore have named them

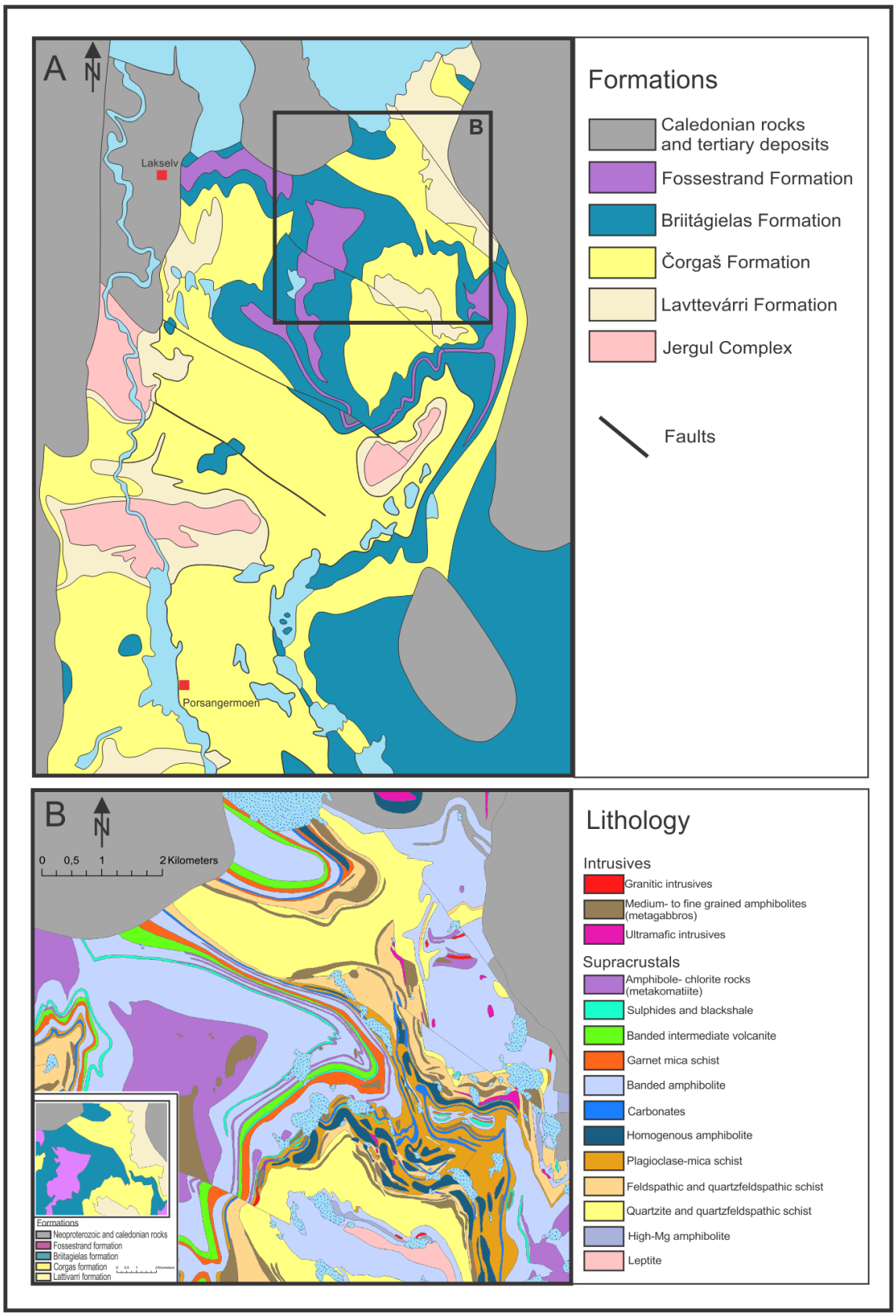

Figure 1.5: A: Geological map of the Northern parts of the KGB (Lakselv Area) showing the different formations (Pharaoh, 1981; Davidsen, 1994; Braathen and Davidsen, 2000; Hansen et al., 2020). B: Lithological map of the Study area (Davidsen, 1994)

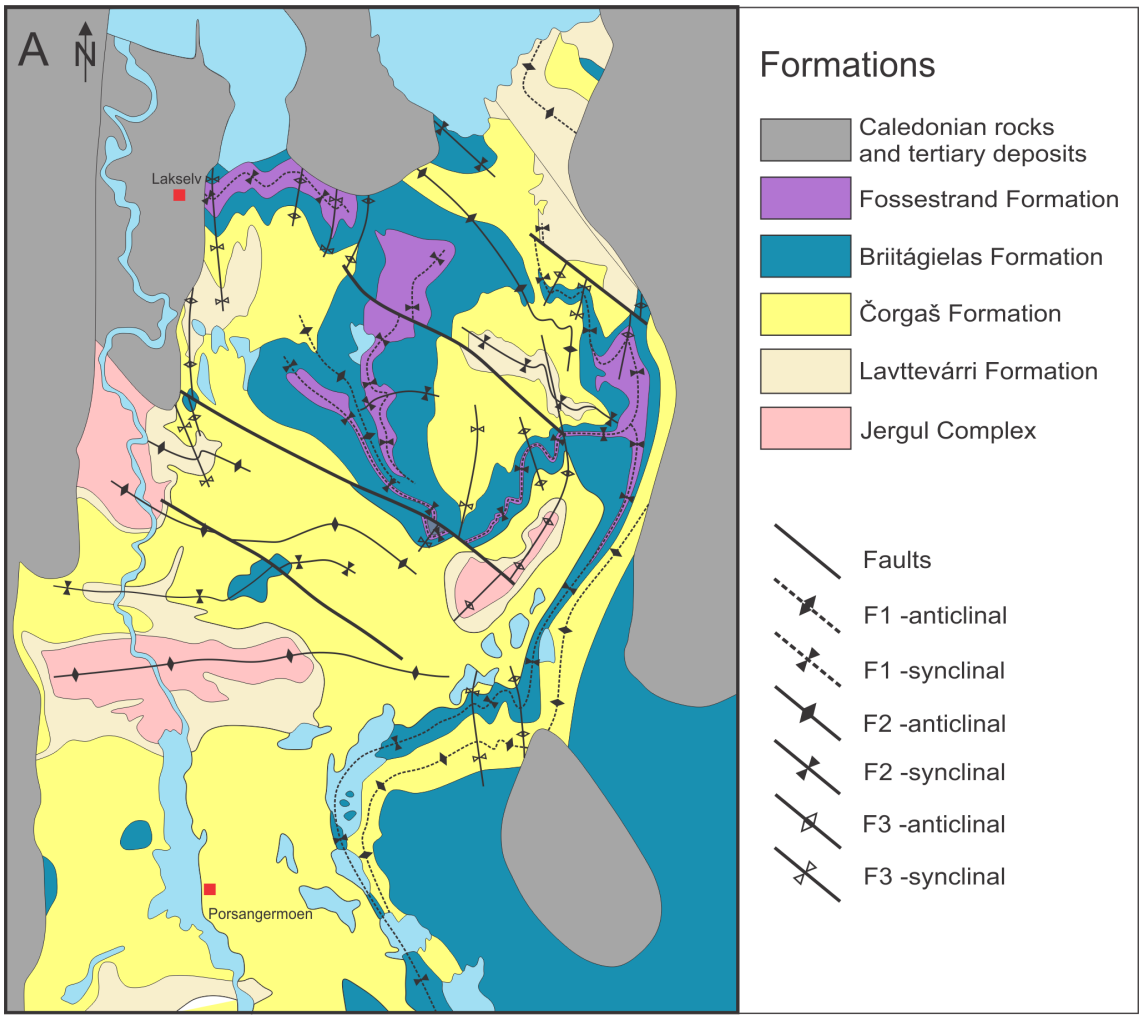

Figure 1.6: Simplified geological map of the Lakselv area with trace of major folds F1-F3 modified from (Braathen and Davidsen, 2000)

D1, D2 and D3. A tectonic model for the KGB has been suggested by (Braathen and Davidsen, 2000)(Fig.1.7).

The D1 phase is characterized by a penetrative east-dipping foliation and mineral banding. The foliation is parallel to sub-parallel with the bedding and therefore S0=S1. According to Braathen and Davidsen (2000), a macroscopic recumbent synform/syncline inverted parts of the KGB. Zones of highly sheared rocks, such as mylonites and blastomylonites occur at the top and base of the belt. These zones are interpreted as regional thrust faults Krill (1985); Marker (1985). The D1 phase is also characterized by amphibolite facies metamorphic conditions based on stable mineral assemblages in metasediments (e.g., kyanite, garnet, biotite) and amphibolites (e.g., garnet, hornblende) (Davidsen, 1994; Braathen and Davidsen, 2000). In the Lakselv area, a major D1 structure, the Brennelva recumbent isoclinal syncline (F1), inverted the whole belt, due to regional E-W contraction (Fig.1.7).

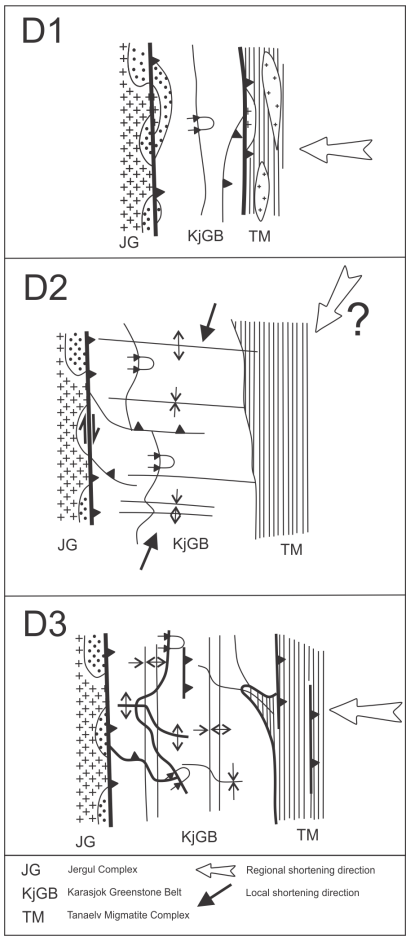

Figure 1.7: Tectonic model for the structural evolution of the Karasjok Greenstone Belt and overlying Tanaelv Migmatite Complex (Braathen and Davidsen, 2000).

The D2 phase is characterized by shear zones located near the base of ultramafic intrusive bodies. In the Lakselv area, the D2 phase is marked by strongly asymmetric shear folds (F2) with vergence towards SW. No major D2 shear zones have been identified in the Lakselv area. Mineral assemblages within D2 shear zones and fold related cleavages indicate retrograde alteration of kyanite, garnet and amphibole into mica, chlorite and quartz, greenschist facies metamorphic conditions during the D2 deformational event (Pharaoh, 1981; Braathen, 1991; Davidsen, 1994; Braathen and Davidsen, 2000).

The D3 phase is most easily identified as S1 foliation that is folded by map-scale folds (F3). The F3 folds are moderately to steeply plunging open, elliptical- to chevron-shaped and either north- or southward plunging. Minor shear zones are visible in ultramafic rocks as well as locally modified fold-limbs. Similar to the D2 phase, greenschist facies metamorphic conditions are suggested for the D3 event (Davidsen, 1994; Braathen and Davidsen, 2000). The complex fold trace patterns within the northern parts of the KGB is shown in figure 1.6.

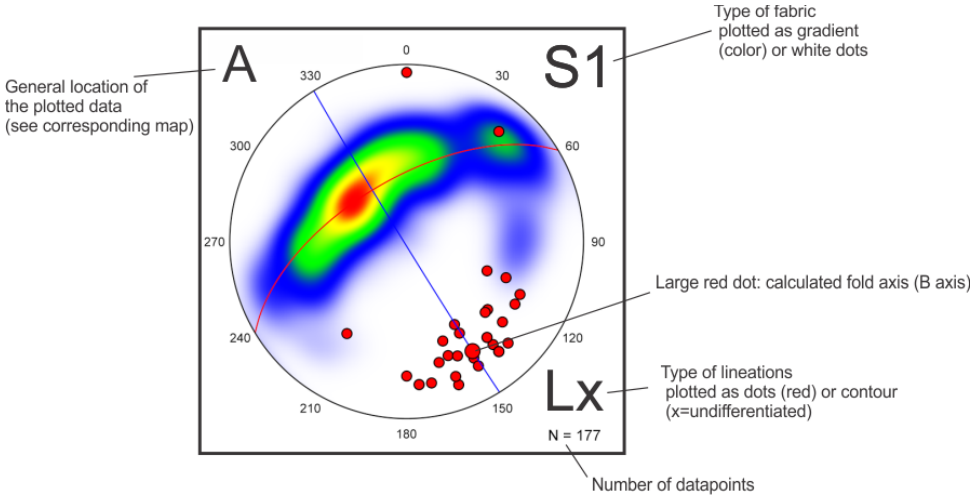

Figure 1.8: Explanation of the stereonets used in this thesis

1.5 Methods and workflow

Six weeks of field work were carried out during 2018 and 2019. The main focus was gathering structural data, way-up criteria and sampling rocks for a thin-section analysis of potentially high strain zones. A total of eight thin-sections were prepared at the University of Tromsø. Due to the lock down of universities during the Covid-19 outbreak, only limited time was available for analysis and interpretation. The structural data will be presented for sub-areas that appear to show distinct structural characteristics for each deformational phase, and areas that show interference of the different phases. Each sub-area is accompanied by maps in different scales as well as semi-schematic cross-sections and southern hemisphere stereonets linked to specific structures within sub-area. Data from location A is represented in stereonet A etc. Structures related to the D1-D3 will also be presented for each sub-area. Due to complexity, some interpretation for each sub-area will be presented in this chapter. Colours and texture for lithology, trace of folds and structural data are used consistently throughout the paper. The information on the stereonets is shown with an example in figure.(1.8)

Chapter 2

Results

This chapter describes the results of the study. The following guidance should be noted: Observed structures have been linked to three structurally different deformational phases (D1-D3). Structures were categorized based on overprinting relationships, fold geometry, lineations and orientation of planar fabrics. However, it is not assumed that these phases are related to three major tectonic events. Therefore, the reader should note that when the notations D1, F1, D2, etc. are used in this study it is not suggested that the KGB has experienced three different orogenies. The notations are only being used as a tool to describe the distinct structures in a precise manner. Determining the history of deformation, whether it is progressive, polyphase or multi-orogenic will be discussed in later chapters. The area investigated lies 4–5km east from the town Lakselv in Porsanger municipality, in northern Norway. The field work covered approximately 10 square kilometers within an area that is somewhat of an anomaly within the northern KGB. Pharaoh (1981); Nilsen (1988, 1989); Braathen (1991); Andreassen (1993); Davidsen (1994); Braathen and Davidsen (2000) have previously identified mostly east-dipping penetrative foliation, east dipping shear zones and west directed thrusting and folding. The area studied in this paper show mostly SW to SE dipping foliation (Fig.2.1). Due to the local variations in both the structures and the erosional cutting effect, the subareas are chosen based on their characteristic map pattern structures (fold interference patterns).

2.1 Structural and tectonostratigraphical overview

Numerous macroscale folds are present in the study area (Fig.2.1), based on variable attitudes of bedding and the main S1-foliation. The Fossestrand subarea, located NW in the study area, display the fold interference relationship between a macroscale, SE-closing F1-fold, refolded by a macro-scale asymmetric SW-vergent F2 synform. The Briittegielás display the complexity of the structures that sits within the

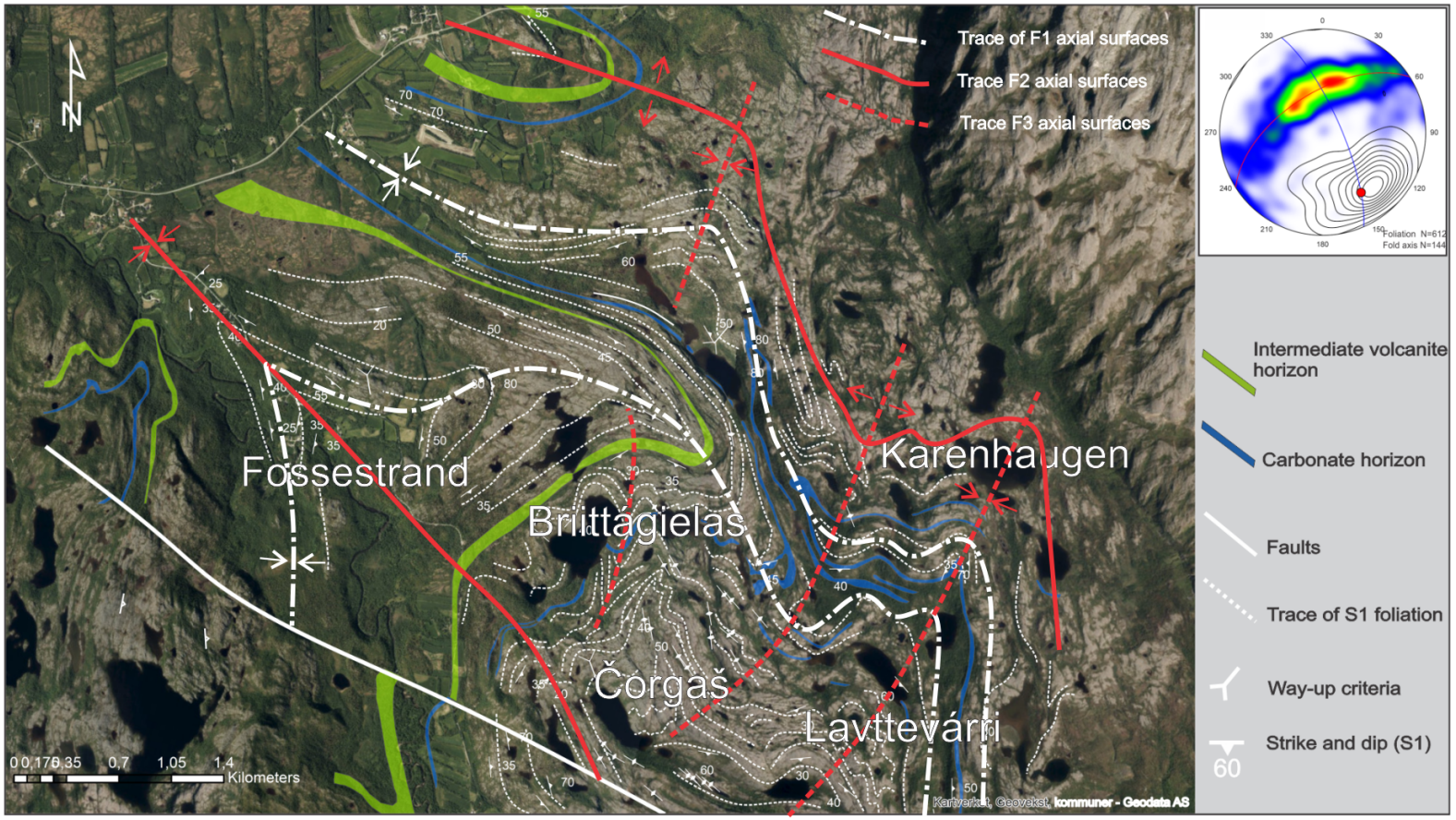

Figure 2.1: Structural Overview map of the studied area, with background orthophoto from www.norgibilder.no. The map show trace of the main penetrative S1-foliation, which is subparallel to bedding (S0), location of subareas, and stereo-net with compiled orientation data for the S1-foliation and L1-L3 fold axis. Interpreted traces of D1- D2 and D3 macroscale folds. Two lithological horizons are displayed based on the work of Davidsen (1994), which is used as a leading horizon for the S0.

Figure 2.2: Way-up criteria. A: Possible cross-bedding in the feldspathic quartzite indicating that bedding is right way up. B: Possible load casts or ripples in a mica-schist indicating right way up (could be crenulations).

F2 synform, later folded by F3. The Čorgaš subarea show the distal effect of F3 folds upon F1 and F2 folds, as well as the F1-F2 fold. The Lavttevárri and Karenhaugen subareas display the most prominent localized D3 structures within the study area, as well as "Ramsey" type 3 fold interference pattern. The general geometry and orientation of structures related to each phase are presented in Table.2.1

Primary structures within the study area are limited, probably due to high metamorphic conditions, strong deformation and the fact that the exposed rocks usually are covered in lichen, thus making the identification of primary structures nearly impossible. However, Davidsen (1994) found several pillow structures within the komatiites in the Fossestrand formation, all showing right way up. Although strong focus on trying to find new way-up structures during field work for this thesis, only two new possible structures were uncovered (Fig.2.2). Both structures sit within the Čorgaš formation although at different areas and different tectonostratigraphic levels (Fig.2.3).

These newly found way-up structures do not correspond with the established tectonic model of Braathen and Davidsen (2000), as the location lies within the proposed overturned limb of the major F1 Brennelva syncline, and thus should be overturned, this will be further discussed in the next chapter.

2.1.1 The Fossestrand subarea

The subarea (Fig.2.4) encompass all the formation except the lowermost, Lavttevárri Formation. In the NE, area D, the quartzitic Čorgaš Formation is overlain by the volcano-clastic Briittegielás- (area F and C) and Komatiite rich Fossestrand Formation (area A and B). To the SE (area E) the Čorgaš Formation is structurally on top of the younger Briittegielás- and Fossestrand Formation. The carbonate

Table 2.1: Overview of structures and metamorphic grade related to different deformation phases and their geometric characteristics

	D1	D2	D3
Fabric (S)	Mineral foliation and banding	Foliation in shear zones, non-physical geometric planes	Crenulation cleavage; foliation in shear zones
Lineation (L)	Mineral stretching	Intersection	N/A
Folds (F)	Isoclinal, recumbent, sheath-like, non-cylindrical	Asymmetric shear folds and kink folds,	Open to tight buckle folds, drag-related
General orientation of S, L and F	S: SW and SE dipping L:SE to SW plunging F: SW and SE dipping axial planes, SW and SE plunging fold axis	S:steeply NE-dipping L:Paralell to dip direction of axial planes and shear zones F:SW-vergence plunging gently to SE & Fold vergence	S:Vertical N-S F:N-S to NE-SE vertical axial planes, initial dip-dependent plunging fold axis
Indications for tectonic transport directions	Foliation and stretching lineations, porphyroclasts and map-pattern	Fold vergence, shear-sense indicators in small-scale shear-zones	Fold geometry, shear-sense indicators in shear-zones and map-pattern
Metamorphic grade	Upper amphibolite facies to amphibolite facies[1]	Greenschist facies[1]	Greenschist facies[1]

[1] Data from Braathen and Davidsen (2000)

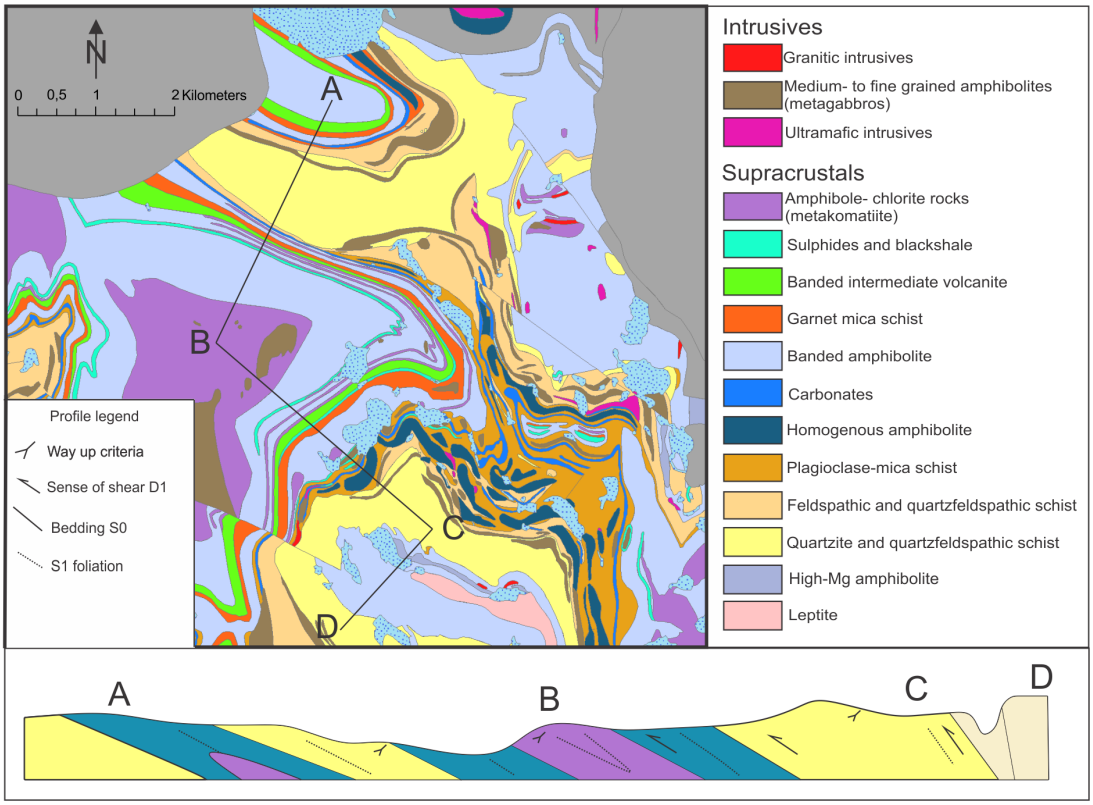

Figure 2.3: Lithological map of the study area. Profile showing general dip of S0/S1, way-up criteria and D1 kinematic indicators.

horizon mark the boundary between the Čorgaš and Briittegielás formations and the intermediate volcanite horizon sits roughly in the center of the Briittegialás formation. There are no tectonic breaks between the formations, or within the subarea.

Deformational structures and geometry — The trace of bedding and S1 foliation is clearly folded (area A-F) and possibly also refolded (area A, B and F) by macro-scale folds. Area and stereonet F, represent the tight to isclinal F1-fold, were bedding is folded and F1 geometry is inferred since bedding on each limb are parallel and dip to the SW.

Besides the macro-scale F1 fold, the D1 structures are seen as well-developed foliation (S1) and banding within the Briittegialás amphibolite, parallel to subparallel with bedding (S0). Mineral stretching lineations are plunging mostly to the SE (L1). Small-scale folds of F1 type are not common in the amphibolite, although some nearly S1 transposed F1-folds have been observed, showing axial plane parallel with foliation and highly varying plunging fold axes. In the highly weathered sulfide zones and komatiites, D1 small-scale structures are preserved (Fig.2.5).

The sharp change in the strike of the S1-foliation, area A and B marks the trace

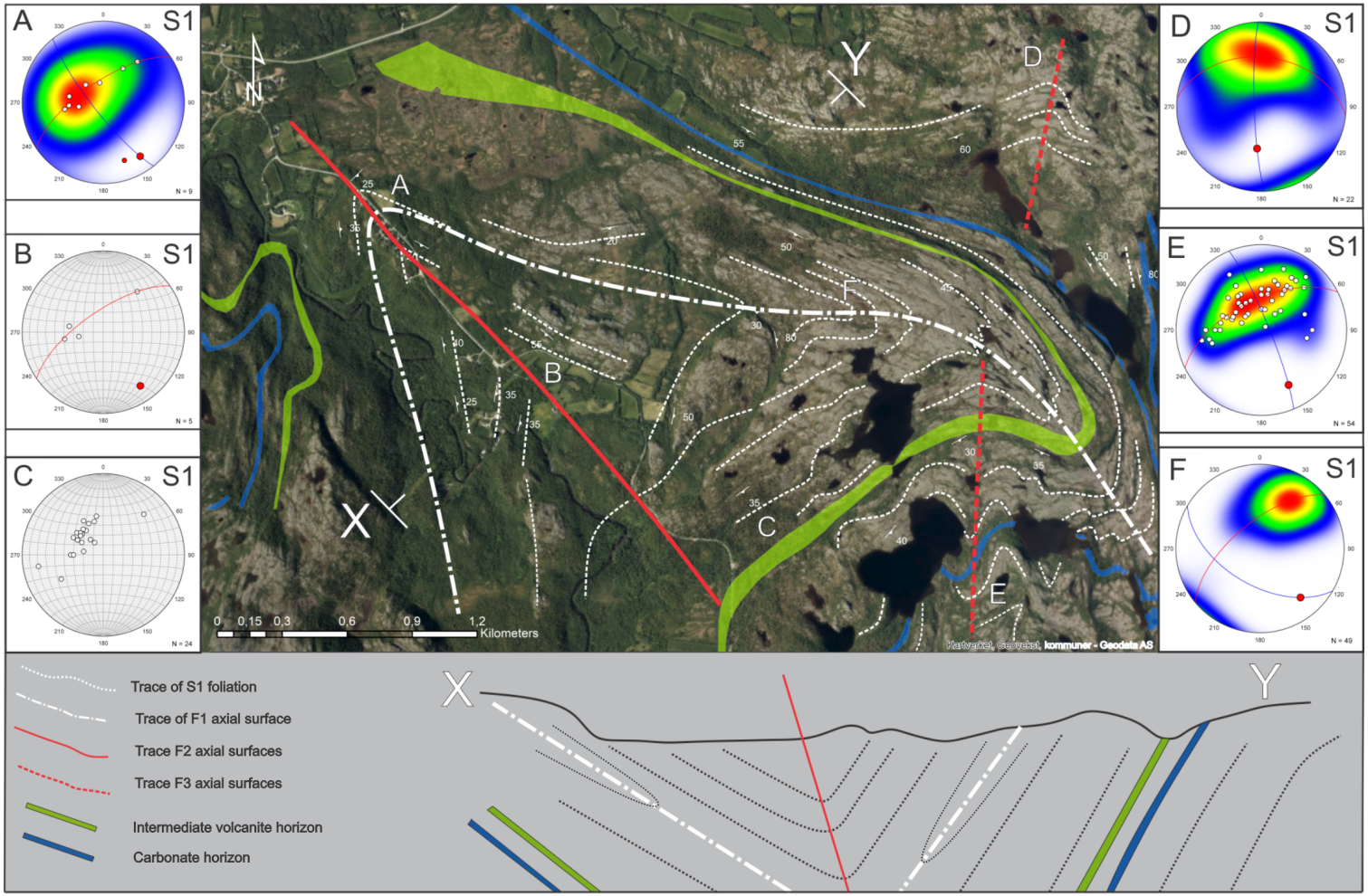

Figure 2.4: Structural map with interpreted cross-section and orientation data in lower-hemishpere stereonets of the Fossestrand subarea, orthophoto basemap from www.norgeibilder.no. Smaller areas marked with capital letters (A-E) denote areas of interest and accompanied stereonets labeled with corresponding letters.

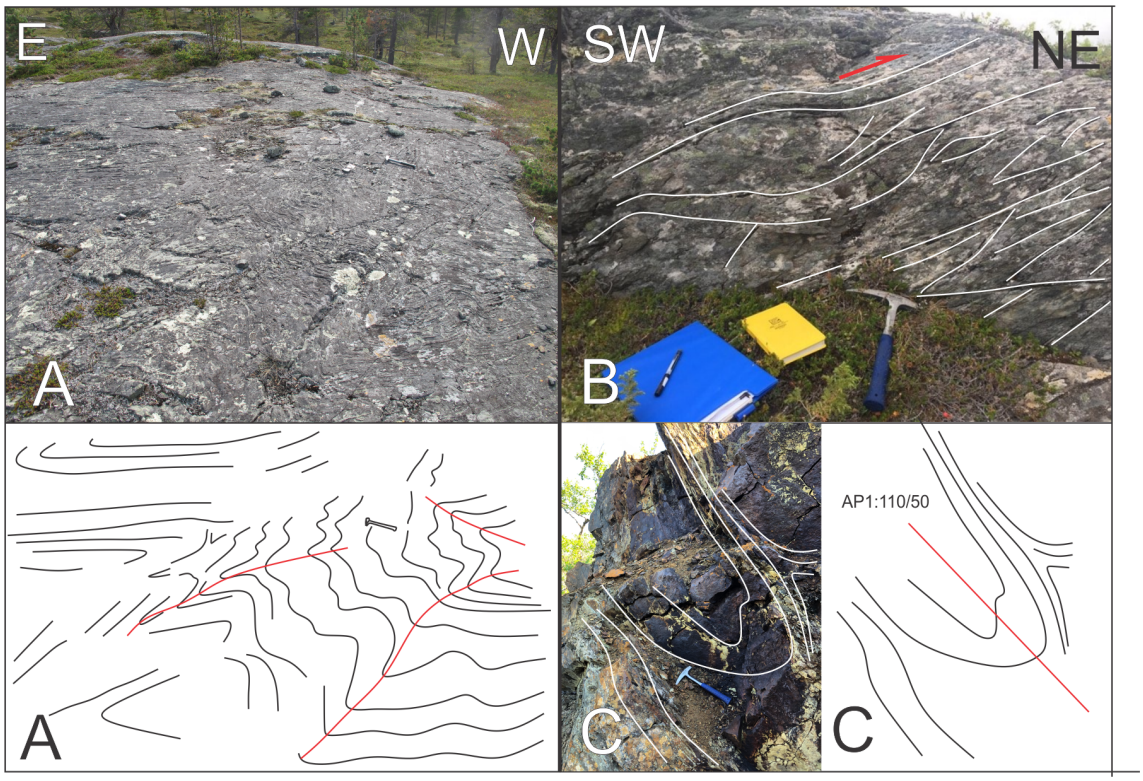

Figure 2.5: D1 structures within the Fossestrand subarea. A: Complex folding and refolding of the banded amphibolite near the F1-F2 interference. B: S-C structures in the komatiite, indicating shearing sub-parallel with S1-dip-direction, top-to-the-NNE near area F. C: Similar-style folds with thickened hinge and thinned limbs-parallel S1-foliation, suggest flow/shear folding along S1-fabrics

of a asymmetric to upright macro-scale F2-synform (Fig.2.4), with NW-dipping axial plane plunging gently to the SE. It also represent the refolding of the macro-scale F1-fold at area A. Small-scale fold-interference patterns and accommodation structures are common near area A (Fig.2.5). Small-scale F2 folds are widespread within the subarea, they display NW dipping axial planes plunging gently to the SW. Compared to the macro-scale F2 fold, the small-scale folds show more gently dipping axial planes and are strongly asymmetric. The main distinguishable feature between the small-scale F1 and F2 folds is the opposite fold-vergence and the asymmetry.

Macro-scale F3 folds are seen refolding the axial trace of the macro-scale F1 fold, area D and E (Fig.2.4). The fold is gentle to open synfrom, N-S striking vertical axial planes, plunging moderately to the south. Small scale folds of type F3 are seen as crenulation folds in the amphibolite (Fig.2.6), accompanied by F2-limb parallel shear zones truncating the S1-foliation.

Interpretation — The Fossestrand area is interpreted to be the core of a macro-scale isoclinal NW vergent F1 synform, refolded by a open, asymmetric to upright SW vergent macro-scale F2 synform. The vergence and initial orientations of the

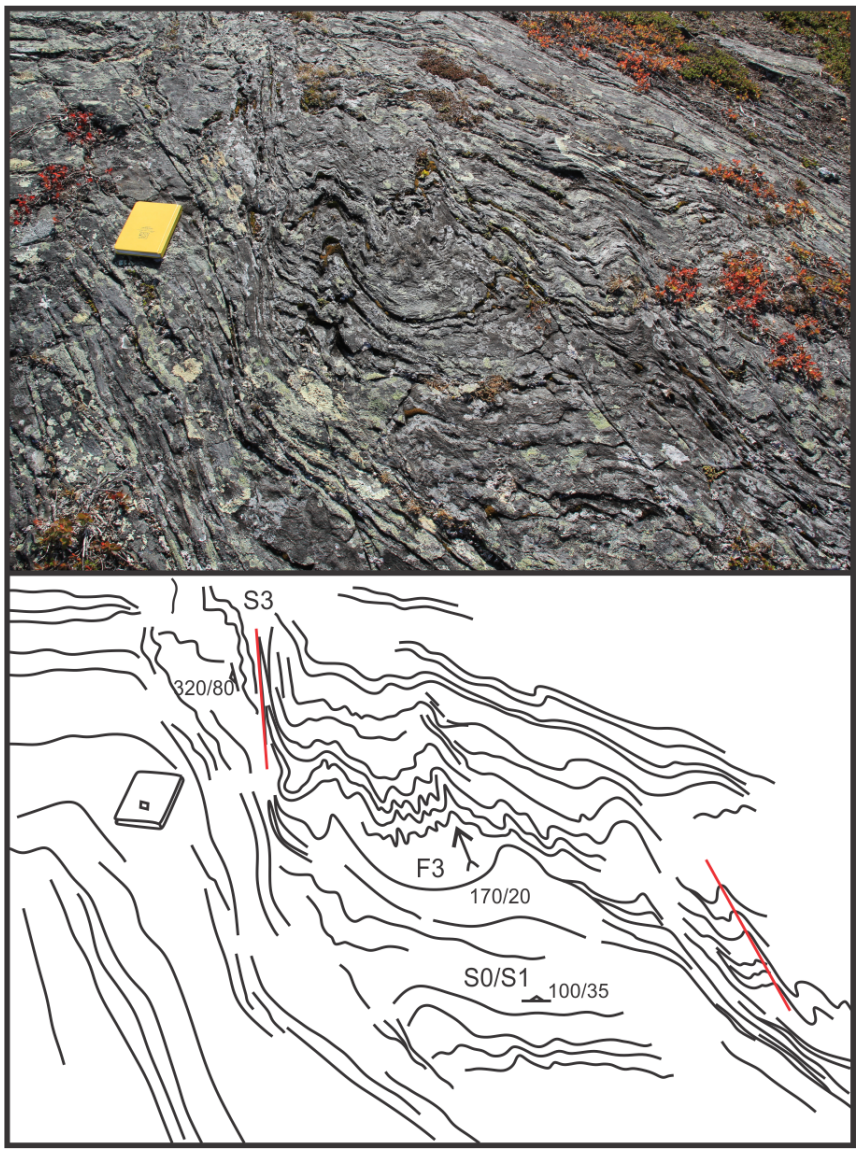

Figure 2.6: Shearing along the limbs of an F2 fold (S2), producing crenulation folds (F3)

F1 fold is inferred based on the relationship between the geometry and orientation of S1, L1, F1 and F2 structures, tectonostratigraphy and the unique map-pattern (Fig.1.5). The D1 structures could thus be a response to NW directed contraction, shearing and or thrusting. This interpretation of the D1 phase does not correlate with D1 phases in other places of the KGB, and thus will be discussed further in the next chapter. The D2 and D3 phases, indicating SW movement based on the vergence and asymmetry of F2-folds, while the D3 phase is represented by gentle to open symmetric folds (F3) linked to localized shearing (S2-S3) in the limbs of F2 folds are consistent with the established tectonic model Braathen and Davidsen (2000).

2.1.2 The Briittegielás subarea

This subarea (Fig.2.7) is dominated by mica-schist, amphibolite, carbonates and quartzite. It comprises the Briittegielás- and Čorgaš formation, where the latter formation is the oldest and sits structurally on top of the younger Briittegielás formation. The subarea show the continuation of the macro-scale F3 and F2 synforms from the Fossestrand Formation. Compared to the previous subarea, folds display shorter wavelength and are far more easily identified in the map-pattern (Fig.2.3).

Deformational structures and geometry — The overall foliation (S1) is parallel to sub-parallel with bedding (S1=S0) except for the homogeneous amphiboles and gabbroic bodies which do not exhibit a well defined foliation. Nevertheless, the shapes of these bodies (Fig.1.5) reflect the local deformation. The macro-scale F1-fold (area F) with axial trace parallel to the main S1-foliation, display an overall NE-vergent isoclinal fold with steep axial planes plunging moderatly to the SE. The western limb of this F1-fold display S-like geometry, while the eastern limb display no additional folding but possible limb-thinning (carbonate horizon). Small-scale F1 folds display similar geometries, although the fold vergence varies from NW to NE (Fig.2.8). The compilation of all the S1-foliation data is shown in stereonet A (Fig.2.7) indicating a macro-scale F2 synform with steep limbs in the eastern parts of the subarea, and more shallow SW dipping limbs west of area F. Thus the macro-scale F1 folds sits within the steep limb of the macro-scale F2-fold, which encompasses the entire subarea see profile (Fig.2.7). Meso to macro-scale folds within the F2-fold (area C-D) shows somewhat different geometry as the macro-scale F2-fold (stereonet A) and the Fossestrand macro-scale F2-synform. The axial planes are steeper and the strike of the axial plane are N-S compared to the NW-SE trending folds in the Fossestrand subarea (F3-folds). The F3-fold geometry changes to a moderately inclined asymmetric fold with axial planes dipping to SE. To the east and west of the same fold, folds with S- and Z-type geometries (area C, D and E) with fold axes converging towards the axial plane of the major F3-fold (area B). These parastitc folds, refolds the western limbs of the macro-scale F1-fold near area F.

Interpretaion — Area F (Fig.2.7) is interpreted to be a F1 isoclinal recumbant fold, refolded by F2, steepening the axial plane and thus appear as an upright isoclinal fold, with NE vergence. Due to the heterogeneous lithology within the Briittegialás subarea competence differences could lead to shorter wavelength parasitic folds and also moving structurally upwards in the stratigraphy the folds will eventually nucleate, thus on a map, with non S1-foliation parallel erosion the trace of the folds disappear. Area B (Fig.2.7), is interpreted to be a F2 shear fold which

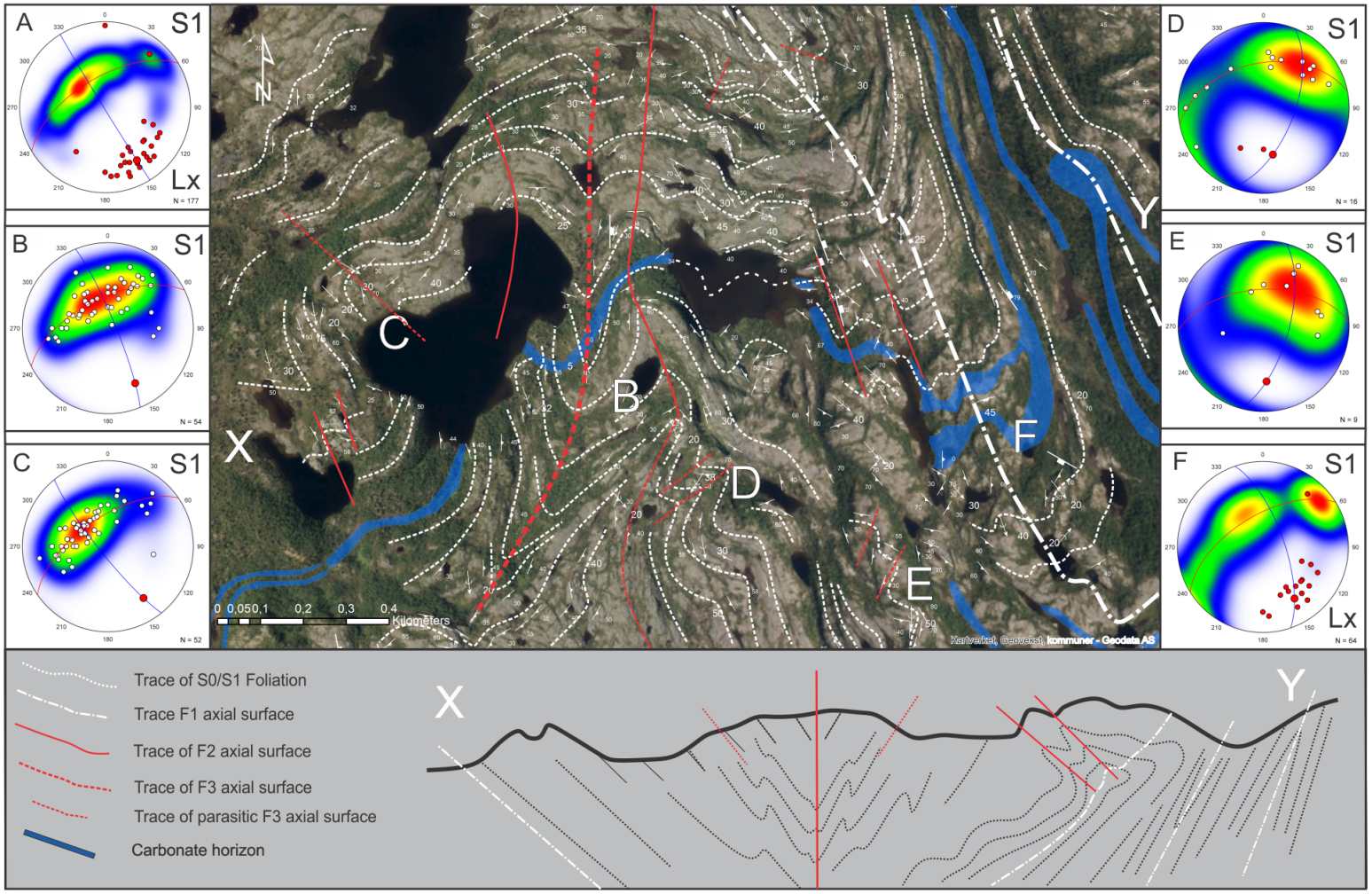

Figure 2.7: Structural map with interpreted cross-section and orientation data in lower-hemishpere stereonets of the Briittegialás subarea, orthophoto basemap from www.norgeibilder.no. Areas marked with capital letters (A-E) denote areas of interest and accompanied stereonets, labeled with corresponding letters.

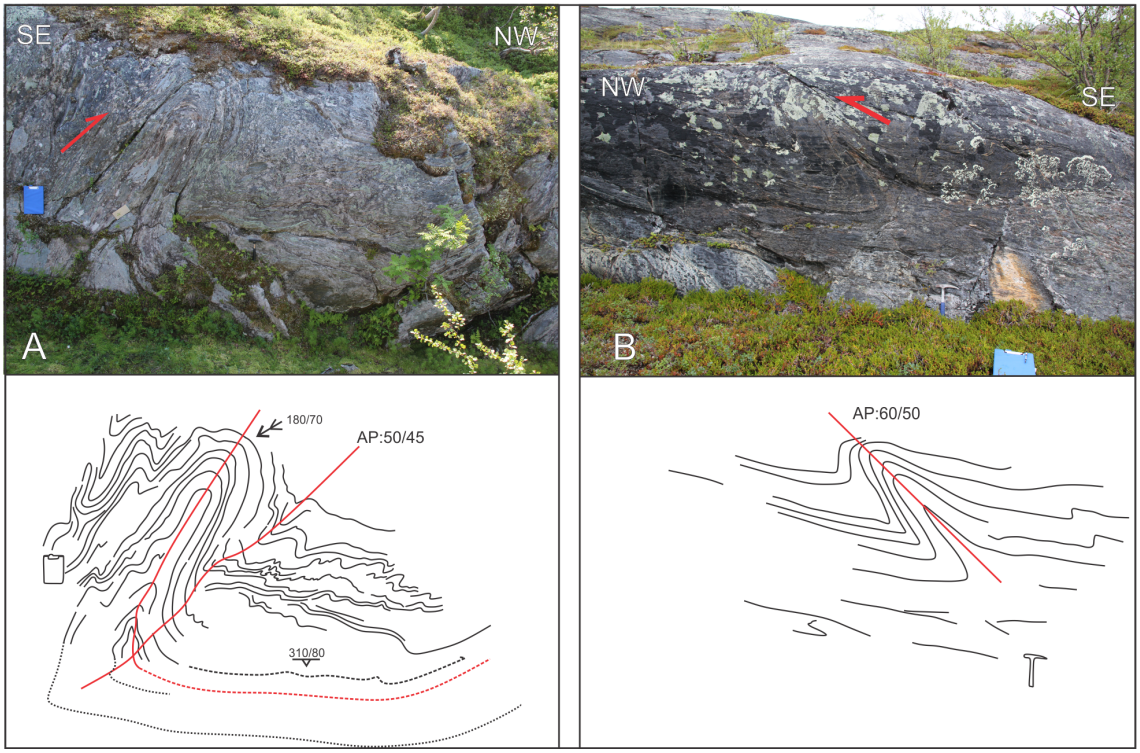

Figure 2.8: A: F1 possible refolded shear fold, showing top-to-NW. Note the fold interference pattern left of the large antiform. B: Shear fold with F2 geometry in the recumbent hinge (outcrop) of an F2 fold.

later rotated into parallelism with the D3 axial plane, tilting the axial plane and producing a large scale fold with S- and Z-type parasitic folds. Complex fold interference patterns and space problems produce folds with atypical geometries and orientations within the core of the F3-fold. Because of the complexity that three folding events produce, the reader should note that simplification of the sub-surface was needed to produce a more easily understood cross-section.

2.1.3 The Čorgaš subarea

The Čorgaš subarea consists mainly of mica rich feltspathic quartzite with well-developed foliation (S1) seen as rhythmic quartz-feldspar- and mica domains. The subarea constitute the Čorgaš- and Lavttevárri Formations and the former formation sits structurally beneath and on top of the latter, indicating that the Lavttevárri is the core of a F1-fold (Fig.2.3).

Deformational structures and geometry — The macro-scale F1 fold, described in the previous subareas merge into parallelism with the axial trace of F2-folds (Fig.2.9) and continues east before turning sharply to the south. Another macro-scale F1 fold is inferred further south, where it is refolded by F2 and exposing the lowermost Lavttevárri Formation area E. The F1-fold geometry are consistent,

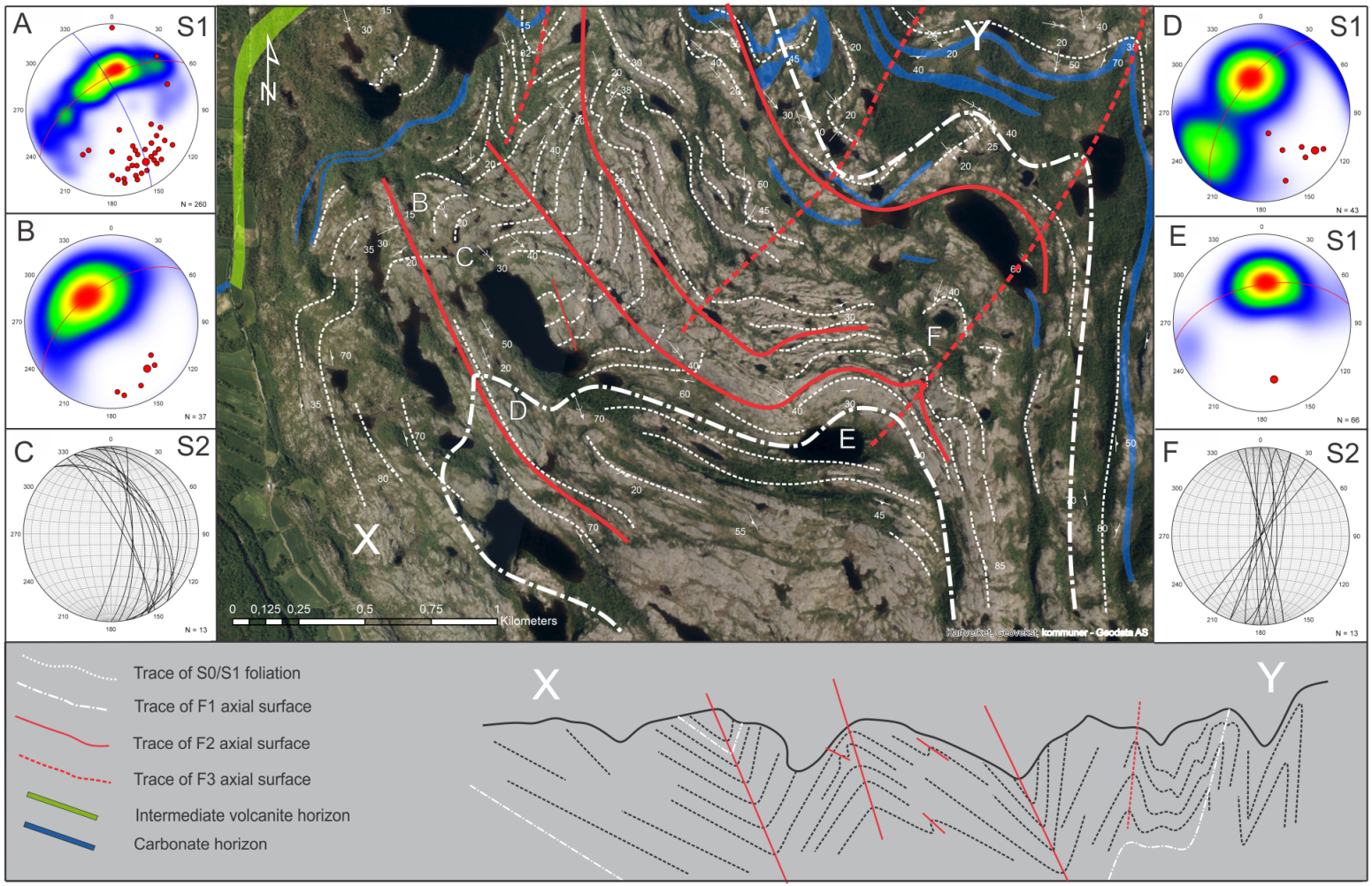

Figure 2.9: Structural map with interpreted cross-section and orientation data in lower-hemishpere stereonets of the Čorgaš subarea, orthophoto basemap from www.norgeibilder.no. Areas marked with capital letters (A-E) denote areas of interest and accompanied stereonets, labeled with corresponding letters.

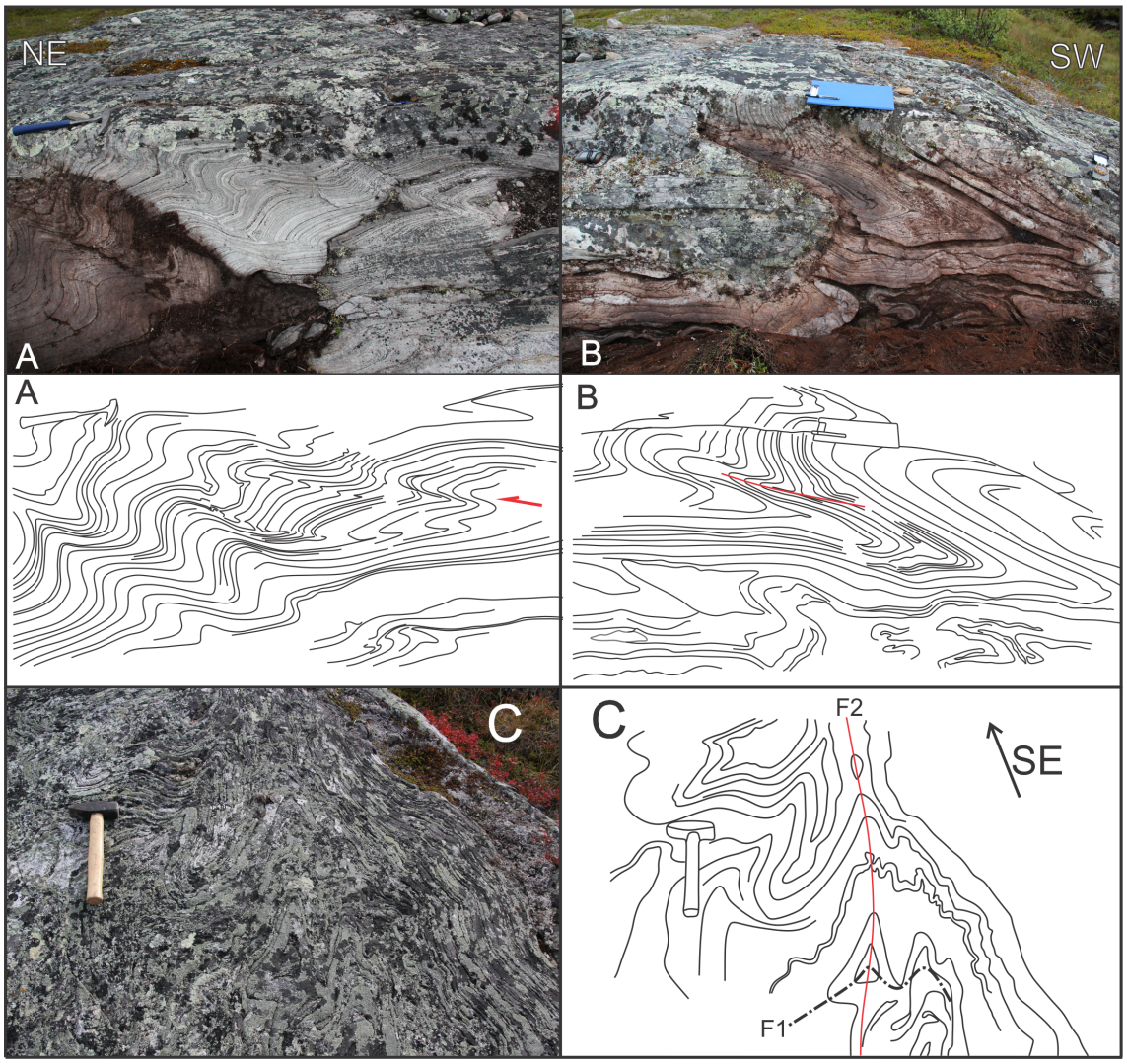

Figure 2.10: A: Local non-continuous shearing sub-parallel with the axial planes of the shear folds (F1-S1). B: Tight recumbent fold (F1) with hinge-collapse, thickened hinges and pinched out limbs. A small shear zone cuts the forelimb and propegate into isoclinal inclined fold (note that A and B is the same locality seperated by approximatly two meters. C: Fold interference pattern of Ramsey type 3 and 2, indicating F1 axial planes dipping gently to SE and F2 axial planes dipping moderatly to NW.

although the orientation varies based on the position relative to the F2-fold. To the west of the F2-axial surface (area B, C and D), the F1 axial planes are dipping gently to the SE and verging to the NW. East of the F2-axial trace, the axial planes of F1 are dipping more steeply to the SW and verging to the NE. Mineral stretching lineations and fold axis (L1) are plunging to the SE. Stereonet A (Fig.2.9) represent the entire subarea and display the macro-scale F2 synform continued from the Fossestrand area to the northwest. This fold is not represented as an axial surface trace on figure 2.9 as most of the subarea is interpreted as the synform, see the trace of F1 axial surface in the profile (Fig.2.9). The geometry of the macro-scale F2 fold is consistent with the Fossestrand F2 fold, displaying steep forelimbs and gently dipping backlimbs. The axial plane is dipping steeply to the NE and plunging to the SE. The meso-scale F2 folds interpreted in figure 2.9, share the same geometry (see profile figure 2.9) and orientations as the macro-scale F2 fold (Fig.2.11) and axial planes are plotted as great circles (stereonet C Fig.2.9). The axial surfaces of the F2-folds are clearly seen refolded (Fig.2.9) by NNE-SSW trending axial surfaces of F3-folds. The F3-folds are gentle to open, moderately plunging to the south (area E and F), these will further be discussed in the Lavttevárri subarea.

Small scale F1 - F2 interference structures are common within the subarea (Fig.2.10 C) indication that D1 produced either NW or SE-vergent folds (F1) (Ramsey, 1962; Thiessen and Means, 1980) later refolded by moderatly inclined folds verging towards the SW (F2). Sub-parallel with F1 axial planes, local shear zones propagate upwards into open, upright, asymmetric kinkfolds (Fig.2.10 A). The geometry of these folds are typical for F2-folds, however the vergence is opposite. This would imply that F2 folds were progressive formed along S1 shear zones during co-axial compression, or that the geometry of F1 folds might strongly vary.

At the base of the quartzite, north of area B (Fig.2.9) a well-laminated mica-schist show foliation with strike and dip perpendicular to the overlying S1-fabric in the quartzite. The foliation is dipping moderate to steep towards NE (S2) (Fig.2.11 B and D) and are sub- to parallel with the axial planes of F2-folds. This would suggest that the D1 and D2 are separate deformational phases.

Interpretation — Indication of dip-slip, top-to-NW kinematic indicators is seen in S1 shear planes (Fig.2.12). Using porphyroclast as independent kinematic indicators could lead to wrong conclusions (Zhang and Fossen, 2020). However, analysis of all the D1 structures and acknowledging the rotation induced by F2- meso and macro-scale folds, the overall dip of planar fabric, plunge of lineations and interference patters, the most likely initial position and geometry of F1-folds would be; isoclinal, near recumbent folds with axial planes dipping to the SE. Also seen in small-scale F1 folds, progressive shearing and folding produce complex structures

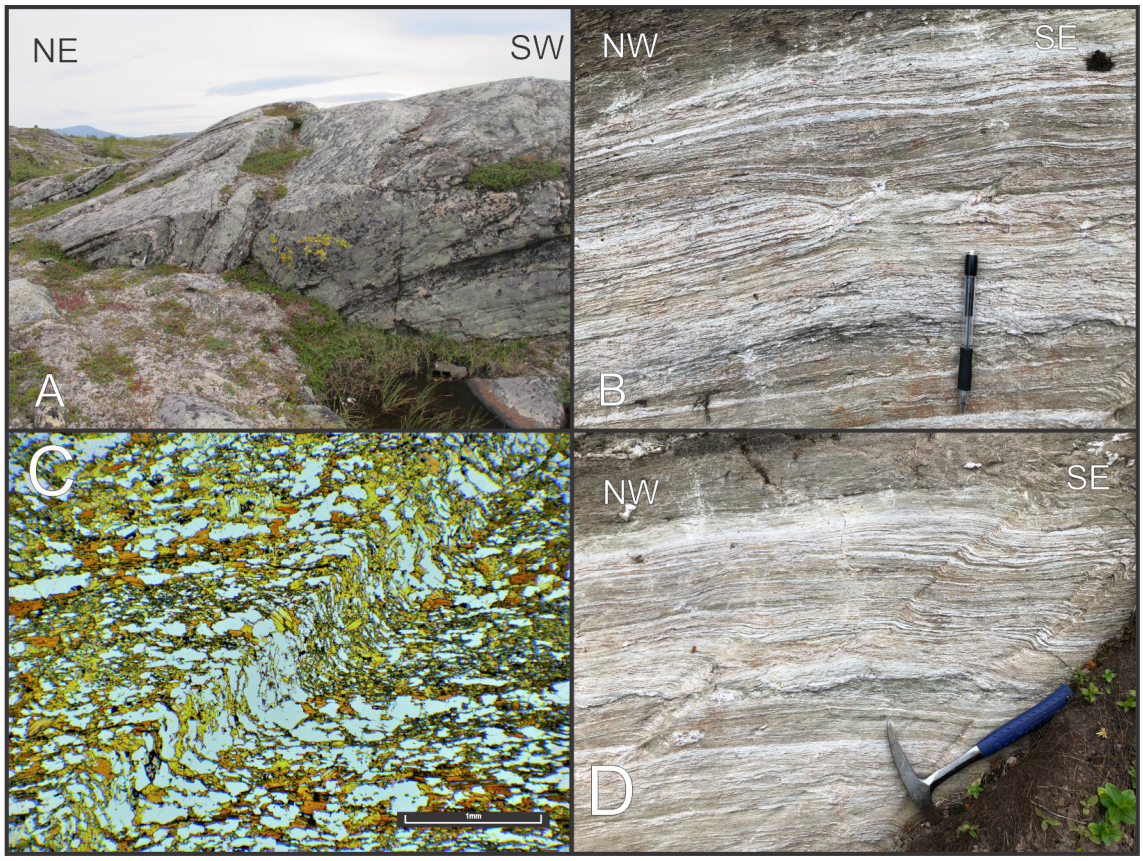

Figure 2.11: A:Overturned asymmetric fold (F2) in the quartzite with axial planes dipping towards NE. B: Thin-bedded mica-schist with transposed S2 foliation displaying boudinage with quartz-infill at the separation gap and asymmetric folds, kink-like. C: Thin section of the garnet mica schist (PPL), foliation defined by the elongation of biotite, showing dextral kinking. D: Same locality as B, dextral kinking displaying kink-planes which are sub-parallel with the general F2 axial planes.

which could be represented in large scale structures, leading to inverted bedding, localized high strain zones, thin limbs and thickened hinges.

2.1.4 The Lavttevárri subarea

This subarea (Fig.2.13) is a close-up and more detailed image of area E in the Čorgaš subarea (Fig.2.9).

Deformational structures and geometry — It shows a prominent macro-scale antiformal fold system with associated synform, and possibly a major axial planar shear zone propagating from limb-paralell S1-trace NW-wards, where it truncates both S1- and S2- axial traces. This suggest that the fold is a F3-fold. Almost parallel with the axial plane of the synform a NW-SE map-scale lineament truncate S1 fabric and appears to displace the bedding with approximately 20 m. Unfortunately, this line also represents an area without exposed rock. Drag-like folds show opposite

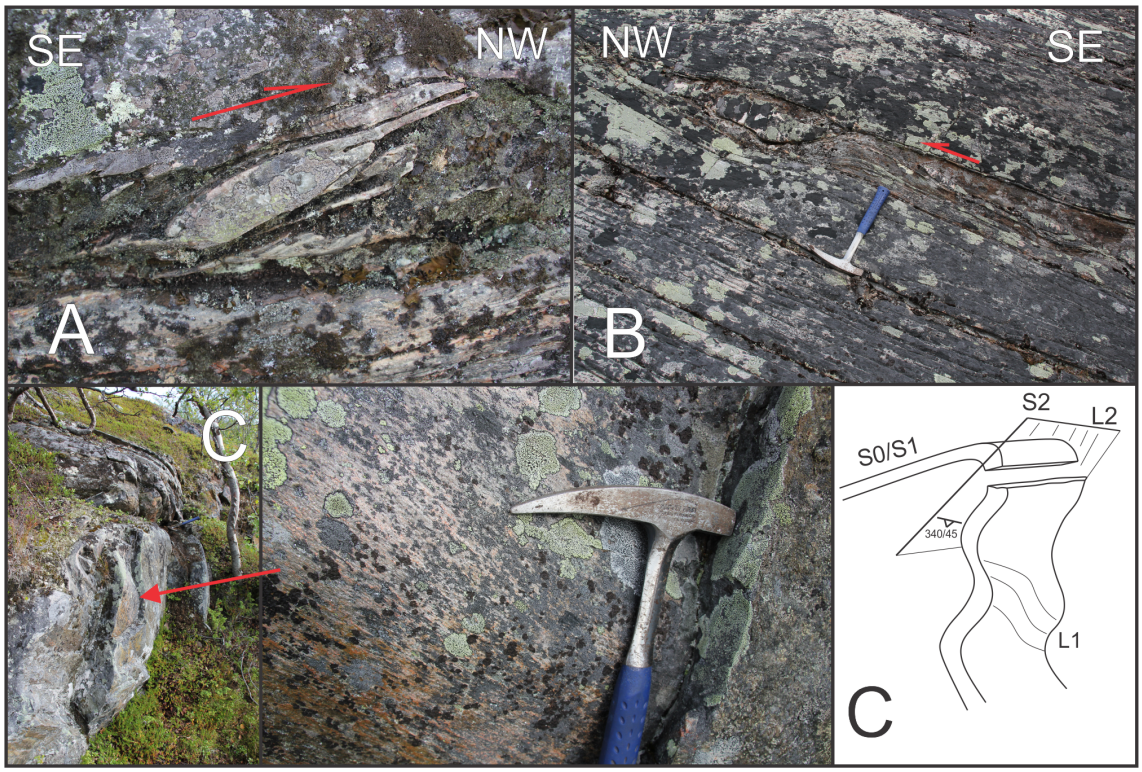

Figure 2.12: A: Complex asymmetric mantled porphyroclast, showing top-to-NW kinematics. B: Boudinaged sigmoidal quartz in a 20-30 cm thick mica-rich layer. C: Asymmetric F2 fold, with NE-dipping axial planes, folded mineral stretching lineations (L1) and stretching lineations paralell to the F2 axial plane dip direction (L2)

vergence on each side of the lineament. The antiform is more open than the synform. The hinge displays fairly shallow dipping S1 foliation, while the backlimb gradually steepens to an almost vertical position. Moving away from the core of the fold, several folds propagate almost radially outwards from the fold core. All the folds show nearly vertical axial planes and moderately to vertical plunging fold axis (F3). The strike of the axial planes shows different directions, from SW-NE to NW-SE (Fig.2.13). At the steep dipping backlimb domain, several shear-folds with vertical NE-SW striking axial planes and S-type geometry are mimicking the geometry of the map-scale fold (Fig.2.14 B). Open to gentle symmetric folds with N-S striking vertical axial planes are more common at the shallow dipping S1 domain (Fig.2.14 B).

Interpretation — The major fold and related axial-planar shear zone are interpreted as D3-structures, since they truncate F1-F2-fold limbs, are closely linked to the main F3-macroscale fold in the Čorgaš subarea (Fig.2.9), have moderately to steeply-plunging axis, and steep axial-planar shear zones. This fold has a map-scale geometry (Fig.2.13) which resembles that of a fault-propagation and/or fault-bend

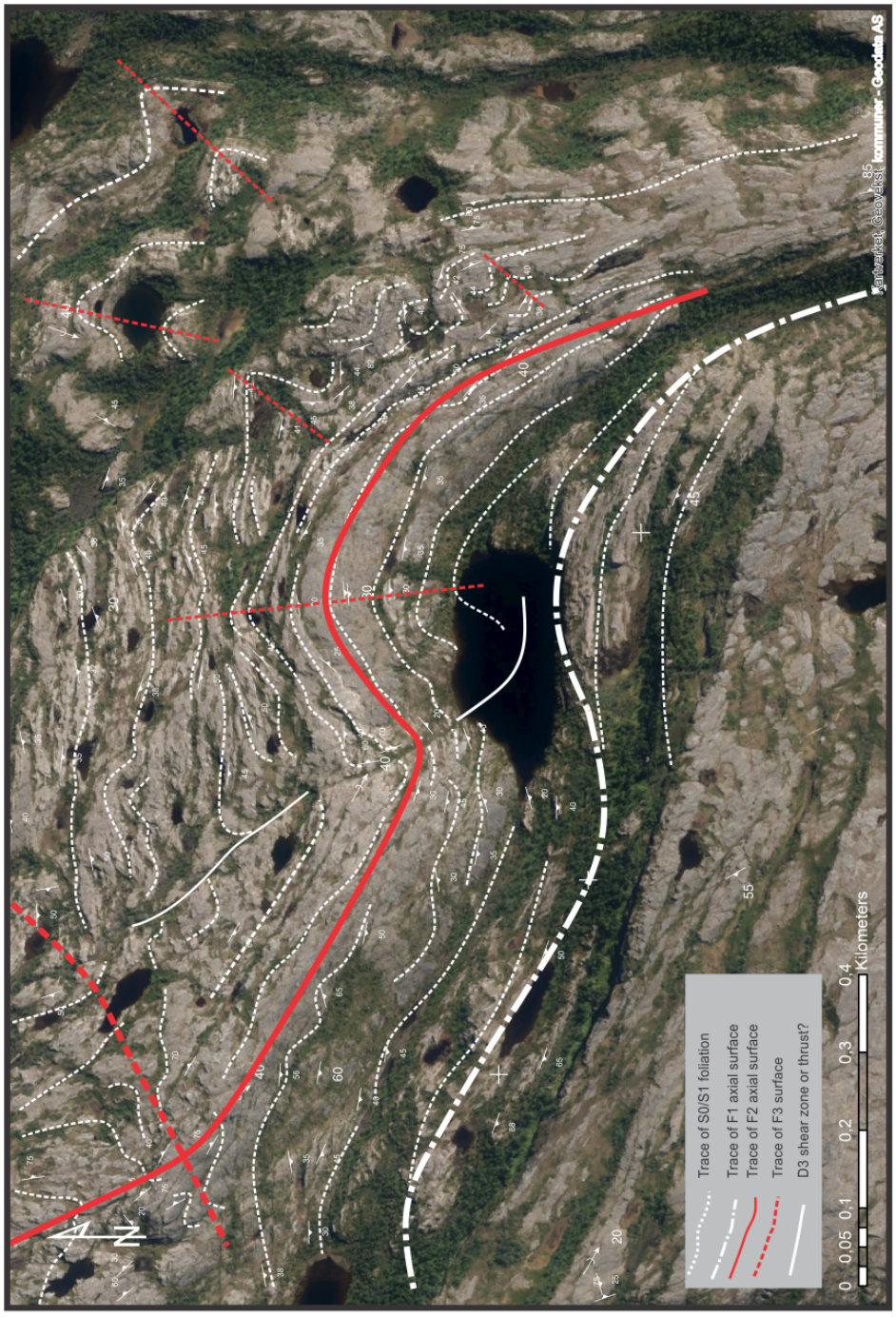

Figure 2.13: Structural map of the Lavttevárri subarea, orthophoto basemap from www.norgeibilder.no

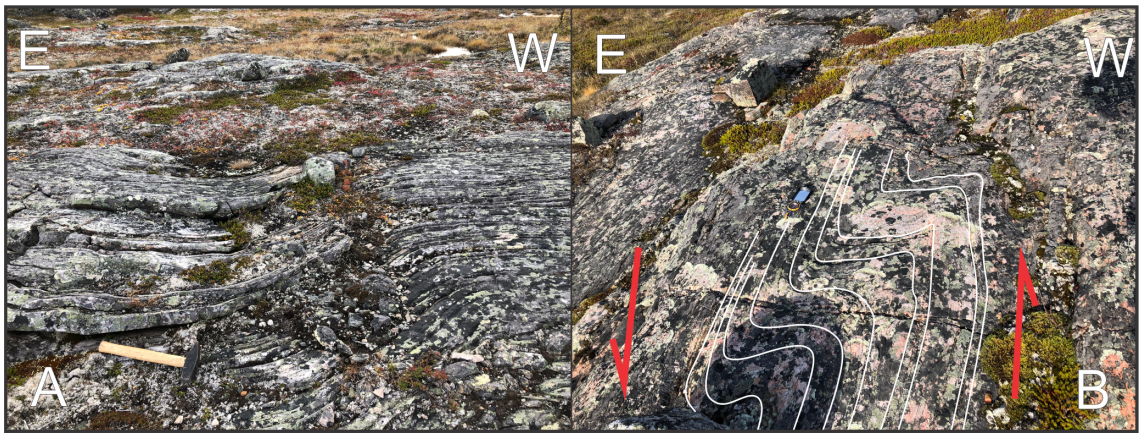

Figure 2.14: Types of F3 folds. A: Gentle to open folds with N-S striking vertical axial planes and gently plunging fold axis. B: Small-scale example of the shear/kink like F3 folds located on the east limb of the macro-scale synform

fold (Dahlstrom, 1970; Jamison, 1987; Jordan and Allmendinger, 1986), or a trishear fault-related fold (Erslev, 1991; Allmendinger, 1998), and may be considered as formed from a potential flat-thrust along S1-foliation into a ramp near the hinge of the fold, and truncates its forelimb. Since the fault truncates its overlying forelimb strata, the fold is more likely generated as a fault-bend fold linked to an underlying ramp-related reverse fault (or thrust), despite no evidence exist that the fault flattens again at higher structural levels (Dahlstrom, 1970).

2.1.5 The Karenhaugen subarea

This subarea is located in the easternmost part of the study area and on the eastern flank of the regional F2-fold traceable all the way from Fossestrand to the Lavttevárri subareas (Fig.2.1). The dominant lithologies are quartzite, amphibolites, and pyroxenites in the Čorgaš Formation and well-foliated amphibolitic schists of the Briittegielás Formation, and several distinct carbonate-rich horizons (marbles), used as stratigraphic markers for the boundary between the Briittegialás- and Čorgaš Formations (Fig.2.3). Each of the limbs of the macro-scale F1-fold (Fig.2.15) consists of rocks which represent the Čorgaš Formation, with the core being the Briittegielás Formation.

Deformational structures and geometry — The major structure in map view is a kink-like macro-fold (likely F3-fold) with sharp hinges and straight, steeply to moderately west-dipping limbs. Orientation data show that the F3-fold is steeply south-plunging and has steep, N-S trending axial surfaces, locally with subparallel, steep west-dipping S3-ductile shear zones (Fig.2.16). On a smaller scale, the main S1-foliation is folded by these macro-scale F3-folds into various dips and dip

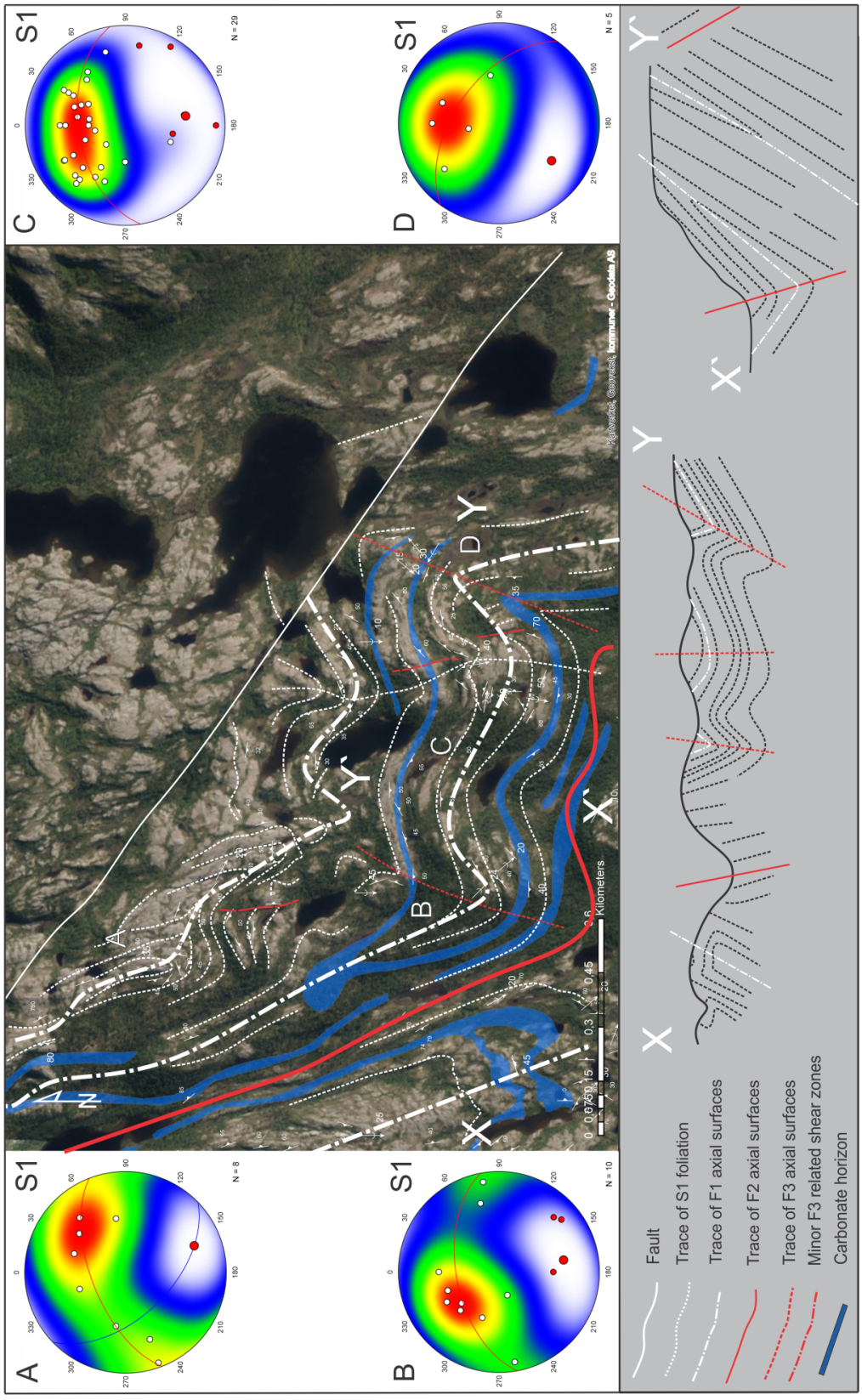

Figure 2.15: Structural map with interpreted cross-section and orientation data in lower-hemishpere stereonets of the Karenhaugen subarea, orthophoto basemap from www.norgeibilder.no. Areas marked with capital letters (A-E) denote areas of interest and accompanied stereonets, labeled with corresponding letters.

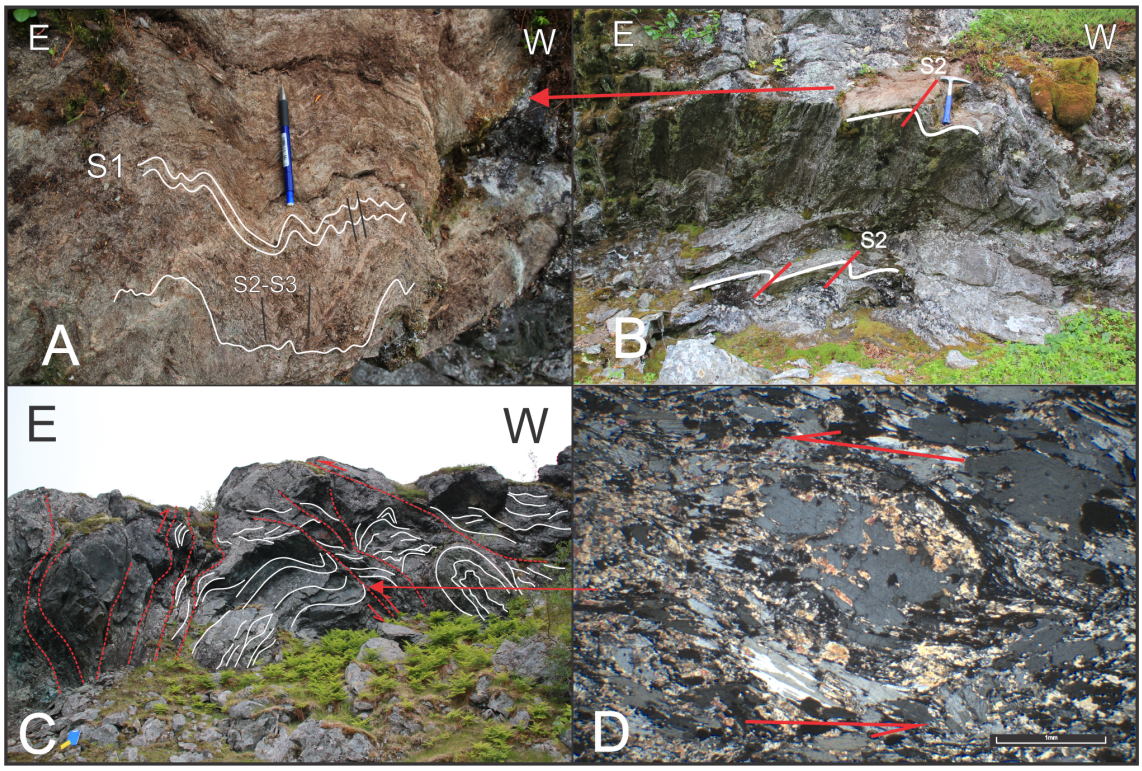

Figure 2.16: Meso to microscale structures within the Karenhaugen subarea. A: Crenulation folds/cleavage possible related to the D3 phase. Upright folds with vertical axial planes. B: Asymmetric west-vergent folds interpreted as rotated F2 folds, although could be F3 shear folds. C: Shear zones localized in the competent pyroxenite, showing steep top-to-west kinematics with an strike-slip component and a possible older set of moderately dipping shear zones with a top-to-E kinematic indicators. D: Thin section showing a asymmetric, later replaced porphyroclast with top-to-E sense of shear.

directions (Fig.2.15 stereonets). The S1-foliation itself is consistently subparallel to the axial-surface of isoclinal F1-folds (Fig.2.15) area A. Further, traces of S1 and S2-axial surfaces are both refolded by the main macro-scale F3-fold, thus supporting the F3-relative age of the fold. Two other sets of presumed F3-folds have been mapped, (i) tight, weakly asymmetric, S and SSE plunging folds with vertical axial planes (area B and D) and (ii) gentle to open S-plunging folds with vertical axial planes (Fig.2.15 C)

Associated axial-planar ductile shear zones are inferred in small-scale, but cannot be directly linked to major shear zones. Anyway, the observed shear zones are steep, and display drag-folds suggesting strike-slip displacement whereas in order areas (e.g. in the mafic rocks figure 2.16) low-angle thrusts are abundant and linked to the same macro-structures.

Interpretation — The major kink-like fold and related axial-planar shear zones are interpreted to be D3-structures, since they refold F1 and F2 axial surfaces and

S1-fabric. The F3-fold is linked to the D3 structures described in the Lavttevárri subarea, and the F3 axial surfaces can be traced to the same area. D3 structures also indicate that both a strike-slip- and dip-slip component were active, as seen in minor shear zones and fold geometry (Fig.2.16).

2.2 Description of geophysical data

Relatively new, airborne geophysical mapping of Finnmark has been carried out as part of the MINN program (Mineral Resources in North Norway), funded by the Norwegian government and run by the Geological Survey of Norway. Comparison of the mapped structures and the magnetic susceptibility is shown in figure (2.17), The anomalies correlate well with the mapped bedrock of Davidsen (1994) and thus the S1 foliation which is sub-parallel to parallel with bedding. Especially interesting is that the interpreted core of the F1-F2 interference pattern is apparent in the geophysical data. The areas that display high magnetic susceptibility, are related to the homogeneous amphiboles, gabbros and komatiites. Since these rocks represent the deformation, the combination of structural data from outcrops in junction with geophysical data is a great tool for further structural analysis of the KGB and other supracrustal belts in norther Norway.

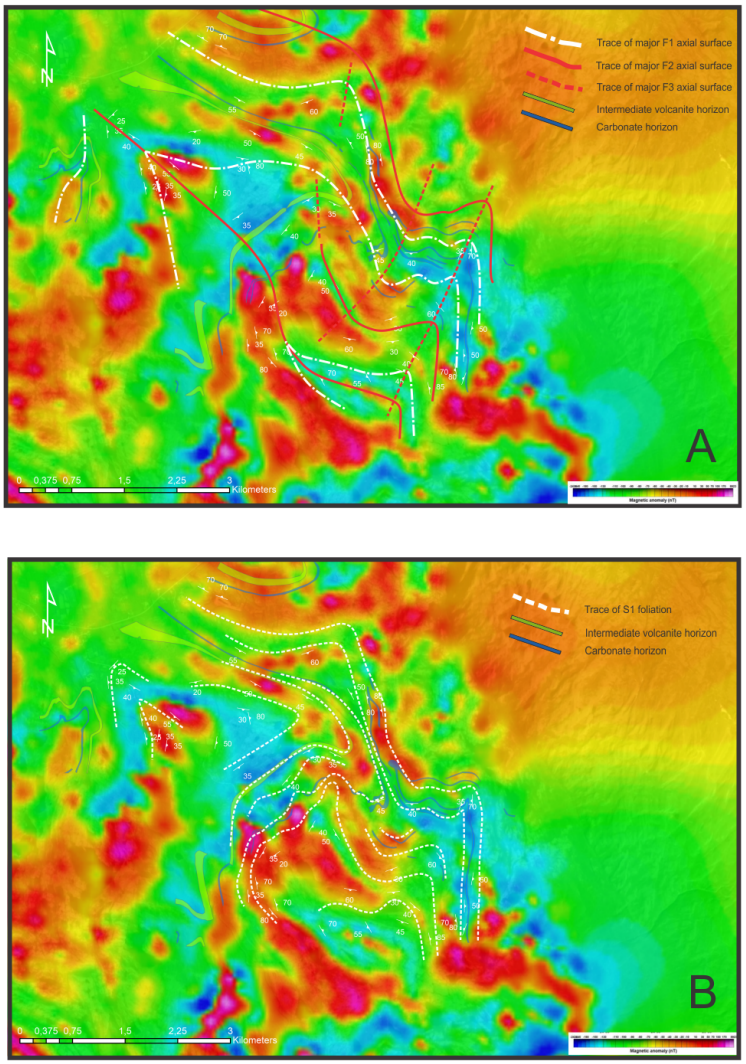

Figure 2.17: Mapped structures on a geophysical basemap (total magnetic susceptibility) show the strong correlation between the magnetic anomalies and structures. A: Trace of fold surfaces F1-, F2-, and F3. B) Trace of S1-foliation. Geophysical data retrived from www.NGU.no.

Chapter 3

Discussion

3.1 Tectono-stratigraphy

Based on structural data and the established stratigraphy which recently has been broadly confirmed by geochronology (Hansen et al., 2020), the formations within the study are out of sequence. This is evident in most of the described sub-areas where the oldest formation lies both beneath and on top of the youngest formation. However, there is no evidence of out-of-sequence thrusting or shearing. This leads to the interpretation that macro-scale isoclinal F1-folds most likely explain the stratigraphic repetition of the formations. In addition, Braathen and Davidsen (2000) suggested that a macro-scale isoclinal recumbent F1-fold is responsible for the stratigraphic repetition in the northern KGB. The studys interpretation of the F1-folds leads to a slightly different tectono-stratigraphy. Based on new way-up structures and new structural data, the D1 phase produced multiple possible fault-propagation isoclinal folds (Poblet and Lisle, 2011) with faults not propagating through the KGB (Fig.3.1).

No overturned structures have been found, which contradicts the proposed isoclinal folding model both proposed in this thesis and in previous work. Overturned folds and misinterpretation of the primary structures may lead to inaccurate or incorrect conclusions. However, based on the contact between the formations it is clear that the lowermost (oldest) sequence sits structurally on top of the younger sequence, indicating either out-of-sequence thrusting, imbrication or overturned large-scale folds. Since no major thrusts have been identified in the field, the preferred explanation is the latter: large-scale overturned folds. A relatively low sample size of way up criteria may explain the lack of overturned structures.

Another question arise as new geochronlogical data proves that the Lavttevárri and possible parts of the Čorgaš Formation were formed prior to the 2.4-1.95 Ga crustal scale rifting events (Bergh et al., 2007; Lahtinen et al., 2008; Melezhik and

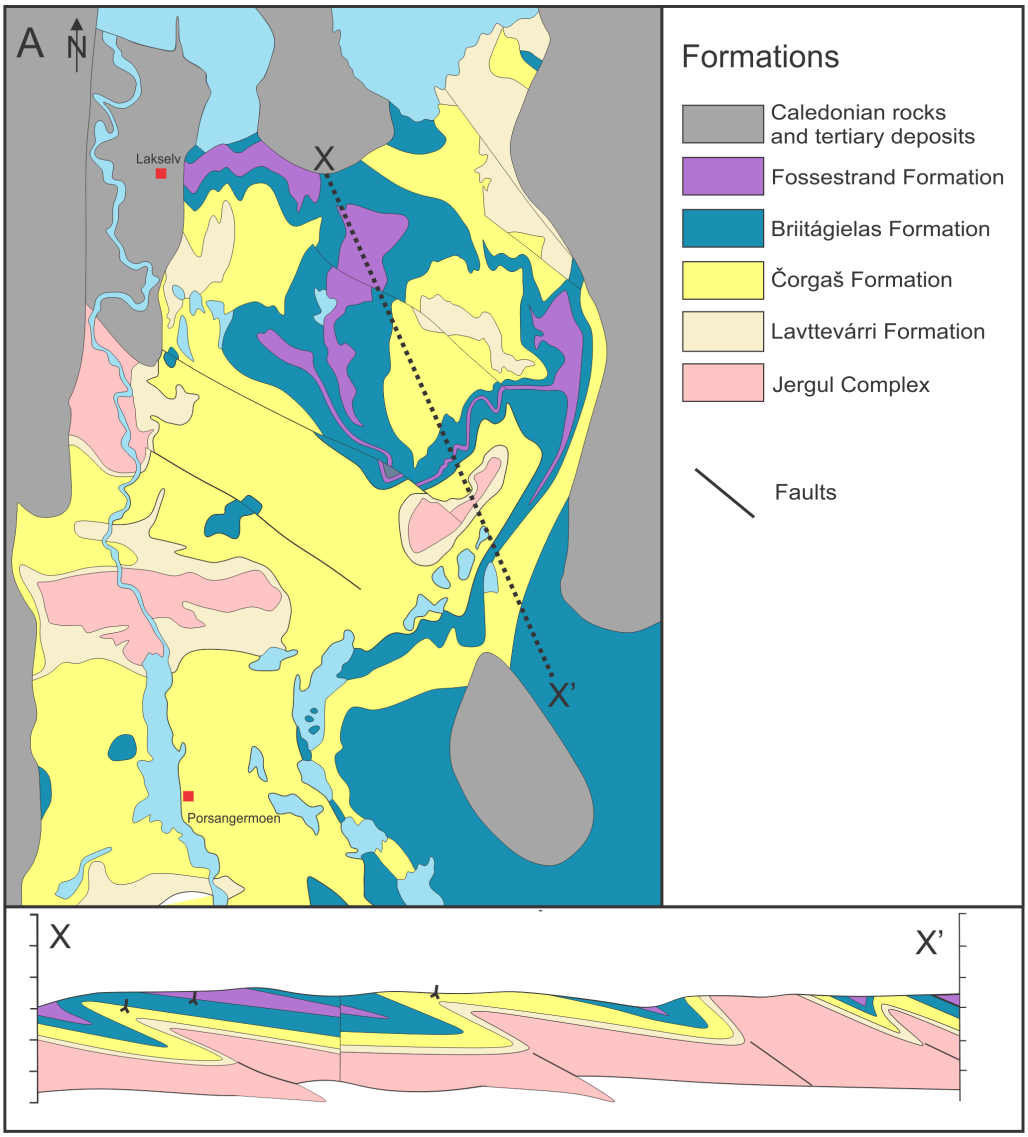

Figure 3.1: Simplified geological map of the norther KGB, showing formations. Schematic profile of the possible "stacking" due to impricate folding during D1 phase. Location of way up criteria from this thesis and Davidsen (1994)

Hanski, 2013) that produced the younger formations in the KGB. One would expect rift-related structures which again could complicate the stratigraphy. However no stratigraphic breaks or unconformities have been identified during field work, although this was not the focus for the study.

3.2 Superimposed structural elements

The nature of the superimposed structures in the KGB makes discussing seperate deformation phases almost impossible. For instance, geometry and orientation of the macro-scale F2-folds is key information for understanding the D1 phase. Therefore, the interpretation of the initial geometry and types of structures before they

were altered by another deformation phase is the key to understand the structural evolution of the KGB. Based on the observed data presented for each sub-area, the related interpretation and discussion of the area will follow. Since the general relationship and superimposed structures seems to coincide in each sub-area, only the most prominent refolding structures will be discussed for each sub-area.

3.2.1 The Fossestrand sub-area

The interpretation that the macro-scale (F1) fold, displayed most predominantly in the Fossestrand sub-area (Fig.2.4) is related to the D1 phase by several features. Both limbs and axial plane of the macro-scale fold are parallel to sub-parallel, which means that the fold is isoclinal. The fold is verging to the NW, which is only seen in isoclinal folds and is plunging gently to moderately to the SE. This change in orientation of dip and plunge, correspond with the refolding of folds with geometry and orientation of F2 characteristics.

The F2-folds mapped in the study area display different geometries and a slightly different orientation than the interpreted F1-fold. The F2-folds are asymmetric open to tight and show SW vergence, opposite of the F1-folds. However, they both show sub-parallel fold axes plunging to the SE, which is interpreted to be caused by rotation of the F1-folds into sub-parallelism with F2-folds.

Asymmetric open to tight folds related to presumed F1-axial plane shearing, as seen in small-scale structures (Fig.2.10), display similar vergence as F1-folds and the geometry of F2-folds and these folds can directly be seen propagating from a D1 structure. Nevertheless, this outcrop represents the problem with categorizing folds with different geometry and vergence into different deformational events, which could be the response of; (i) initial back-thrusting during D2 producing opposite vergence folds with both asymmetric and isoclinal geometry (Krabbendam and Leslie, 1996; Humair et al., 2020), (ii) local strain-partitioning during the D2 phase as a result of high competence differences within the KGB (Carreras et al., 2013), (iii) accommodation structures near the hinge of the macro-scale F2 fold may produce non conform folds related to D1, D2 and D3 phases.

Despite the fold ambiguity related to the different phases (D1-D2) and the lack of chronological data on the different structures, the isoclinal, NE-vergent folds (F1) were produced earlier than the asymmetric open to tight SW-vergent folds based on fold interference patterns and overprinting relationships (Fig.2.10, 2.11 etc).

The initial orientation of D1 structures and their tectonic interpretation is complex due to multiple refolding phases. Based on the overall dip-direction of the northern KGB (E, SW, SE and W), the large number of E and SE plunging lineations and the unique shape of bedding which corresponds to refolding with per-

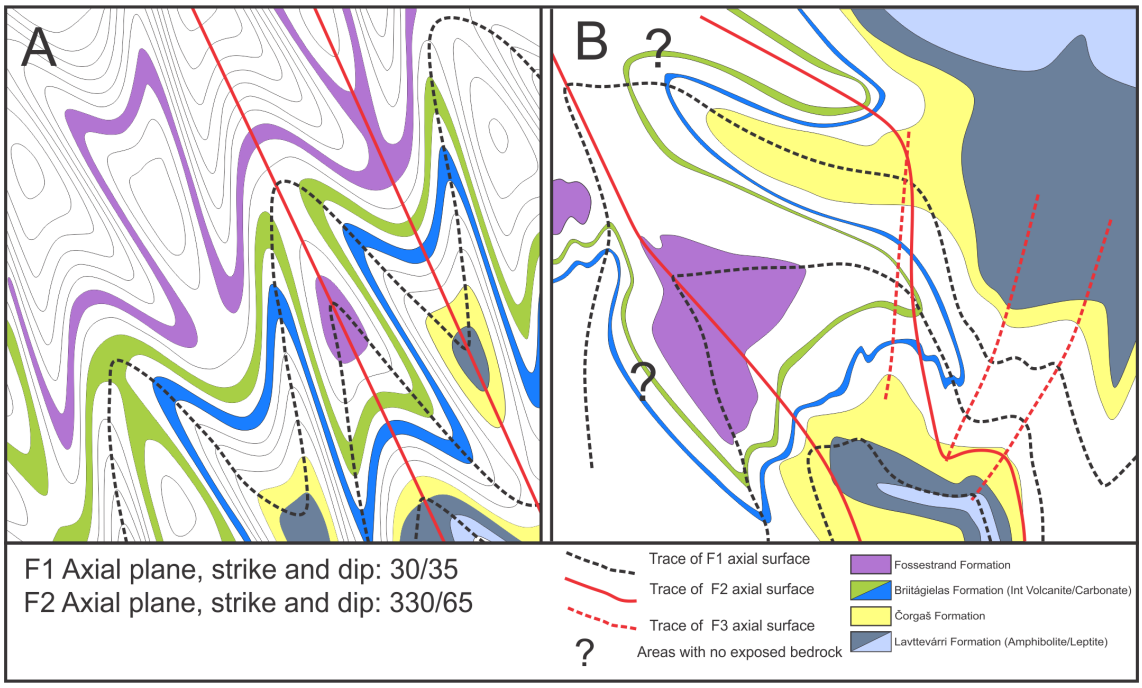

Figure 3.2: A: Ideal interference pattern on a horizontal plane, with symmetric, cylindrical folds based on a matlab script developed by Martin Schöpfer. B: Study area showing interpreted axial surfaces of F1, F2 and F3 folds and the general map pattern based on Davidsen (1994).

pendicular axial planes orientations (Ramsey, 1962), the first fold indicate that the initial axial plane were striking to the NE and dipping gently to the SE, and a second fold axial plane striking to the NW and dipping moderately to steep to the NE (Fig.3.2). Due to the relatively small impact of F3-folds on the F1-F2 interference pattern, the similarities with a nearly ideal Ramsey type 3 interference pattern is evident.

This interpretation of the F1-F2 refolding does raise certain problems. Some areas do not have exposed rocks and thus some lithological boundaries are extrapolated (see the difference regarding the Fossestrand Formation in the geological maps Fig.3.2 and 3.1). The area investigated does not include the western part of the macro-scale F2 folds which is thought to be the cause for the refolding. Therefore, the interpretation of axial surfaces west in (Fig.3.2) is purely based on the lithological boundaries. Further, the interference pattern suggests that D1 were produced by NW-SE shortening or thrusting. This has not been observed anywhere in the KGB by other authors. Nevertheless, the data collected in the study area suggest NW vergent F1-folds as well as NW kinematic indicators in D1-structures. A comparison between the interpreted structural evolution of the Fossestrand sub-area and the established structural model based on the work of Braathen and Davidsen (2000) for the KGB is shown in Figure 3.3.

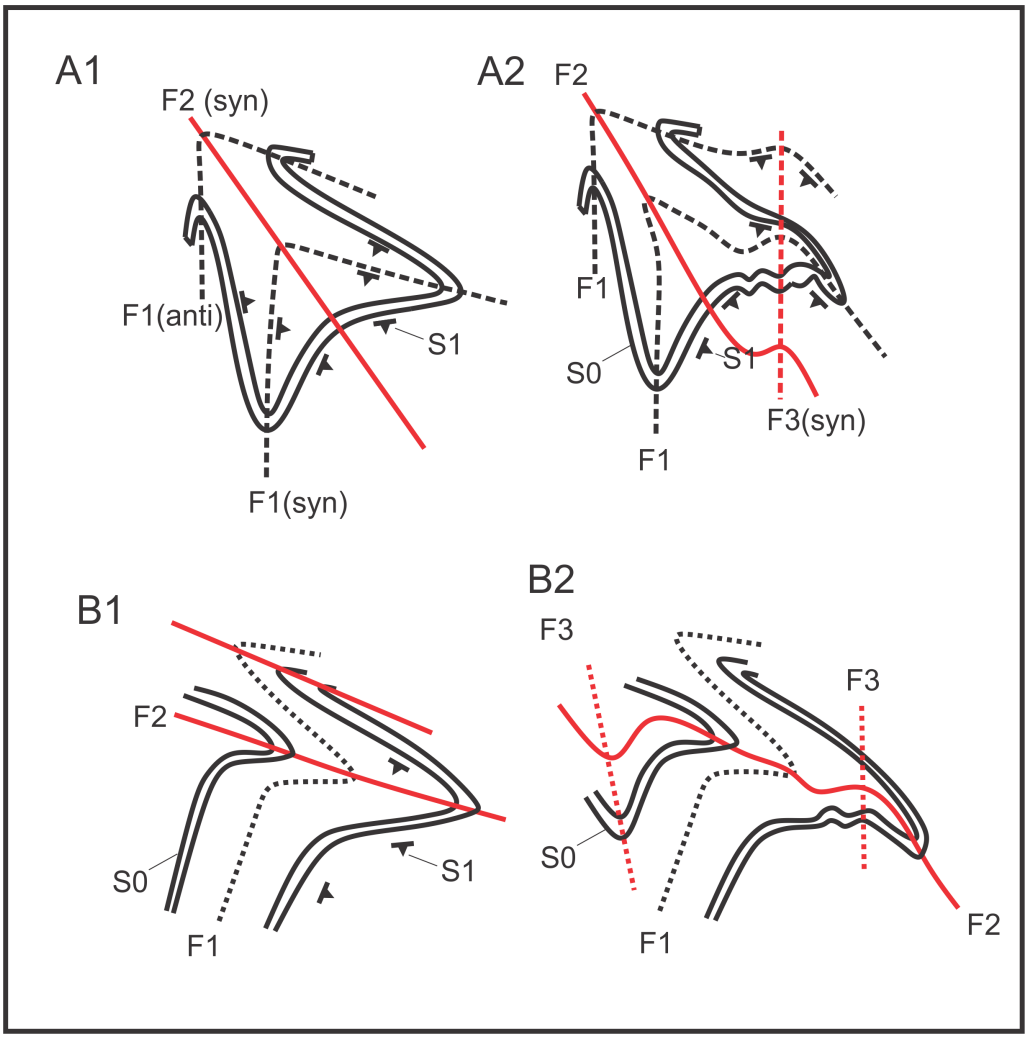

Figure 3.3: A possible evolution of the Fossestrand/Briitágielas complex folding pattern A: This thesis, B:(Braathen and Davidsen, 2000). A1: F1-F2 Ramsey type 3 fold interference pattern. A2: F3 rotation and refolding of F1-F2. B1: F2 refolding F1 obliquely and thus not producing an end member refolding pattern such as A1. B2: F3 refolding F1-F2 folds.

3.2.2 The Čorgaš and Briittegielás sub-areas

The D2-D3 refolding relationship is easier to interpret due to the wast difference in fold geometry and easy to follow macro-scale axial surfaces in the map pattern between the two phases (Fig.2.9). However, when introducing the macro-scale F1-folds the situation becomes more complex. Structural data obtained from the Briittegielás sub-area (Fig.2.7) show the most complex and diverse folding within the entire study area. The Briittegialás sub-area represent the merging of all three macro-scale folds seen as sub-parallel axial surfaces (Fig.3.3) B). The complexity is interpreted to be the result of high competence differences within the Briittegielás Formation due to the heterogenous lithology. There is also geometric contrast between the meso- and small-scale F2 folds in the sub-area. The meso-scale folds display moderately to

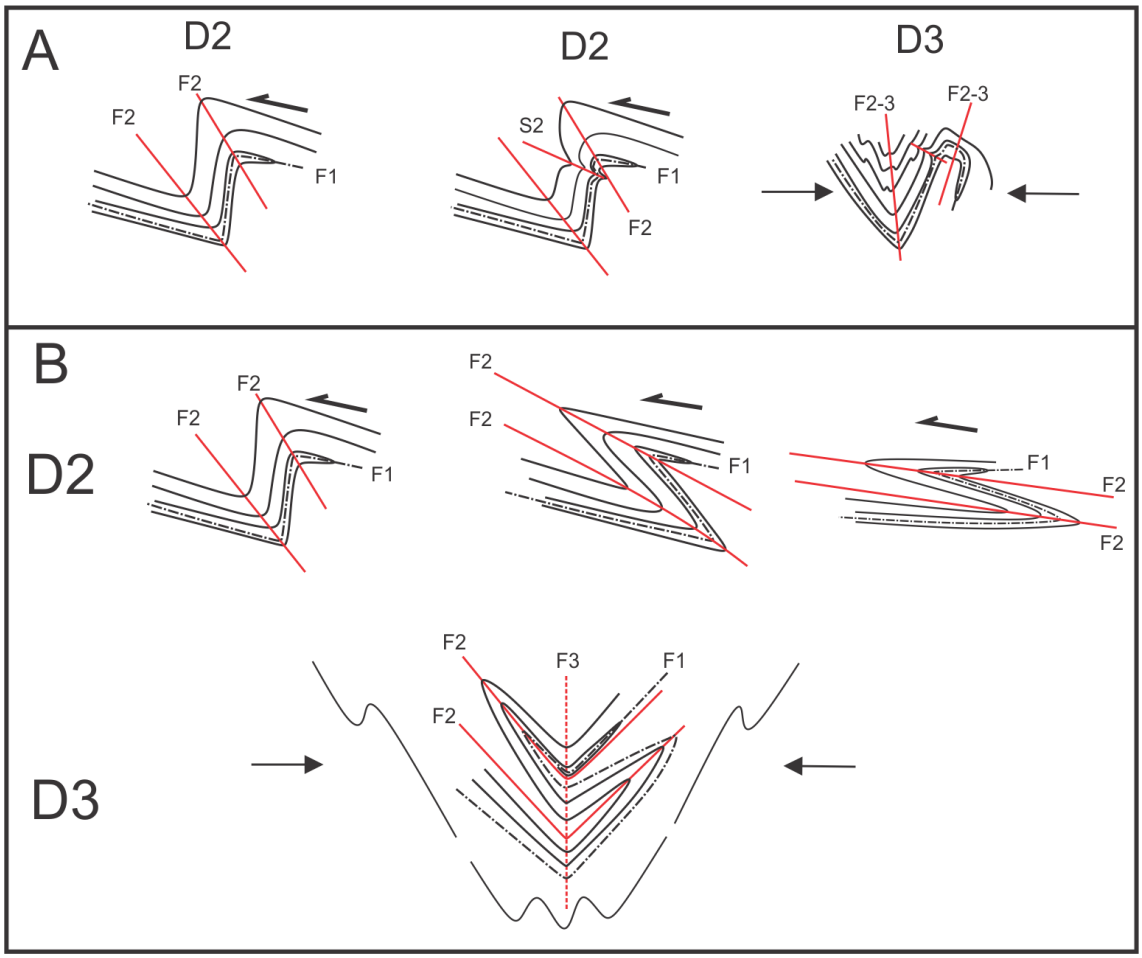

Figure 3.4: A: Possible polyphase evolution of the D2-D3 evolution of the Briittegielás synform. B: Possible progressive evolution of the Briittegielás synform, D2 represent a gradually tightening and almost transposed S2 foliation, D3 refolds the near horizontal F1 and F2. (Figure A represents the best model for the macro-scale structures, while figure B best represents the small- to meso-scale structures, thus the possibility of scale-dependant structures are present.

steeply dipping axial planes, while small scale folds are highly asymmetric and some overturned and nearly recumbent (Fig.3.4). Both lithology and scale are important when relating folds to the D1, D2 or D3 phases.

3.2.3 The Lavttevárri sub-area

The Lavttevárri sub-area does not exhibit a typical refolding interference pattern, this could be the result of relative high changes in elevation within the area compared to the otherwise rather flat exposed rocks in the other sub-areas. As mentioned in the tentative interpretation in the last chapter, the macro-scale F3 fold is assumed to be a fault-propagation fold (Jamison, 1987) or a fault-bend fold (Jordan and Allmendinger, 1986) produced by a major fold and related D3 axial-planar shear zone, which is sub-paralell with F2 axial planes (Fig.3.5).

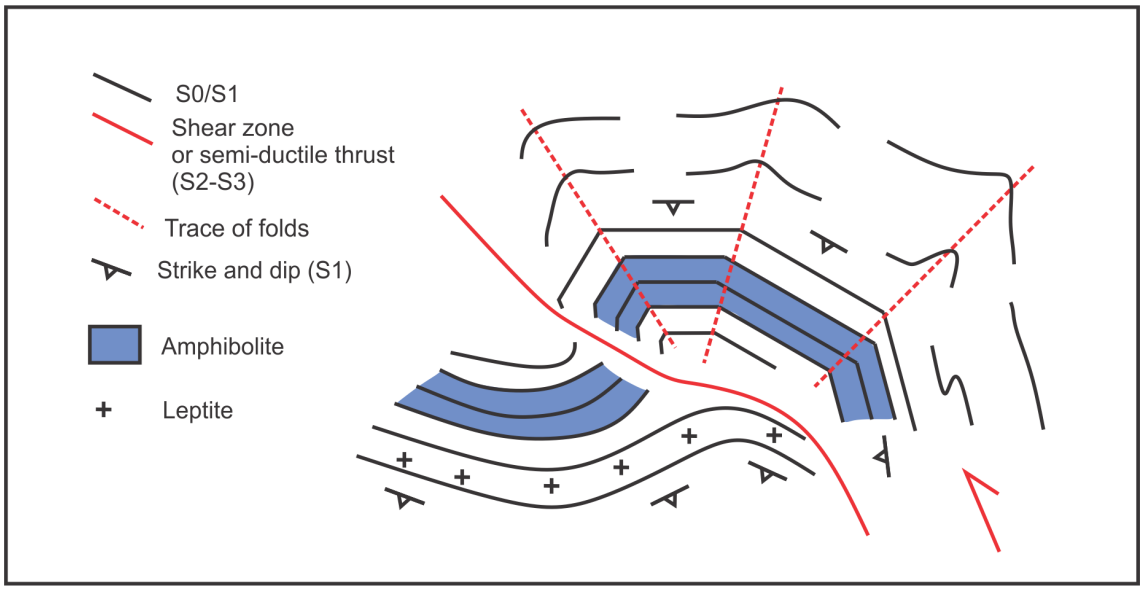

Figure 3.5: Interpretation of the Lavttevárri F3 fold. A: Possible fault-propagation fold, showing general dip of S1, displacement of S0 and axial traces of related folds.

There are alternative options for explaining the temporal relations of the fold: i) The fault-propagation fold is a D1-structure, which formed when the sedimentary package was horizontally and unfolded. Thus, representing a reverse-thrust with top-to-NW movement and a non-plunging fold, later folded and rotated into the gently to steeply plunging fold and sub-vertical thrust and shear zone. The problem with this interpretation is that these structures refold existing D1-D2 structures which can be explained by reactivation of the previous thrust during transpressional (D3) regime. ii) Sinistral NW-SE orientated strike-slip fault and shearing produced a "vertical" fault-propagation fold sub-parallel with the F2 axial planes in the later stages of D2, thus deforming earlier D2 structures. (iii) Different strike and dip of S1, due to F2 folding affects the geometry of the F3 folds (Strain partitioning). In the steep N-S to NW-SE limbs of F2 folds, F3 folds appear as asymmetric shear folds with vertical axial planes and vertically plunging fold axis. The more moderately to gently dipping S1 in the F2 back-limb, with dip direction perpendicular to the local shortening direction, produce open moderately dipping symmetric folds (Fig..

Despite several possible interpretations of the formation and the relative age of the structure, the data show that folds related to the possible fault-propagating fold is refolding both D1 and D2 structures and additionally, the geometry and orientation of the structures suggest E-W contraction accompanied with localized and relative small-scale shear zones which are both trending N-S and NW-SE.

The interaction of D1 and D3 structures are well represented in the Karenhaugen sub-area (Fig.2.15). The map pattern is similar to a Ramsey type 3 interference pattern, suggesting that the two folds had sub-parallel to parallel trend and near

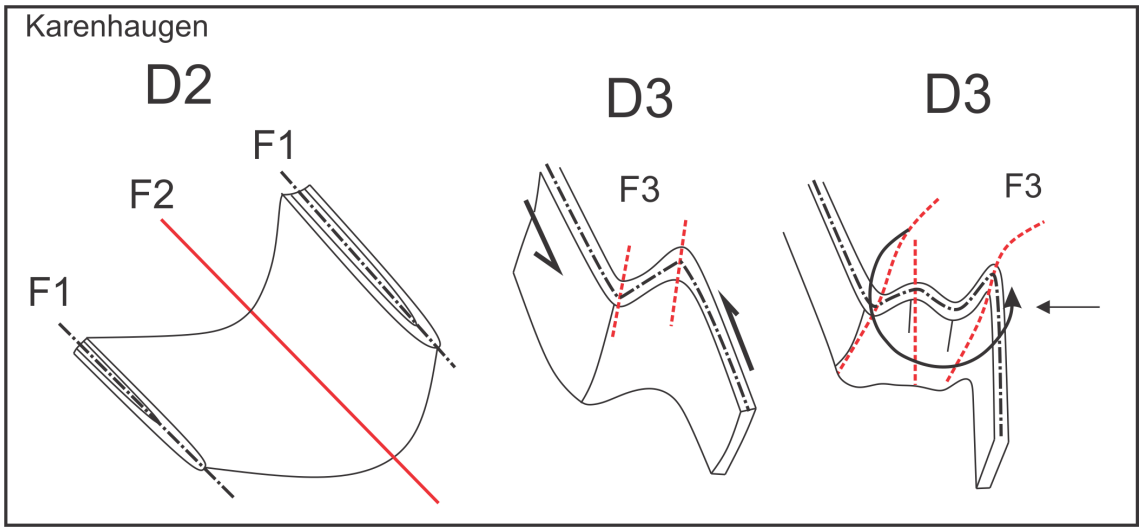

Figure 3.6: Interpretation of the structural evolution of the Karenhaugen area. D2:F1-F2 folding producing steep to moderatly dipping F1 axial planes in the forelimb of the macro-scale F2 fold. D3: Shearing along the F2 limb causing rotation and paired shear folds. Continued shearing, thickened hinges and internal competence differences caused the layers to rotate synthetically with regards to the layer parallel shearing causing local strain partitioning, modified to fit the Karenhaugen sub-area based on Carreras and Druguet (2019)

perpendicular dip of the axial plane (Ramsey, 1962; Thiessen and Means, 1980; Grasemann et al., 2004). However, this does not suggest that the F1- and F3-folds shared a contractional direction, but rather that after D2 refolding, the F1-folds were trending N-S to NW-SE. The map pattern, combined with data describing the F3-folds suggest that the folds were produced by a localized sinistral shear along the steep limbs of macro-scale F2-folds (Fig.3.6), thus producing polyclinal folds usually associated with progressive deformation (Carreras and Druguet, 2019).

3.2.4 The Karenhaugen sub-area

Although the structural model for the Karenhaugen sub-area and therefore the D3 phase suggest that strike-slip shearing or at least a strong shear component was active, no major shear zones have been found during field work. Also, the appearance of two types of folds related to the D3 phase (symmetric and asymmetric) is interesting and could be the result of misinterpretation F3 folds with F2 folds, although the tectonic model (Fig.3.6) tries to explain this. The two fold types, both categorized as F3 folds, might suggest that the asymmetric F3-folds were produced first by sinistral strike-slip to oblique shearing, and later normal E-W contraction due to a possible shift from a transcurrent to a transpressive regime. This sequence of events is usually reversed, where the continued contraction eventually leads to a shift to either a transpressional or transcurrent regime (Burg and Podladchikov, 2000).

Also symmetric structures do not necessarily exclude the presence of a ductile shear zone (Mukherjee, 2017). Similarly to the Lavttevárri sub-area, data suggest an E-W contraction with localized shearing sub-parallel with F2 and F3 axial planes.

3.2.5 Polyphase vs progressive deformation

Categorizing structures into phases (D1-, D2-, etc) purely based on orientation and geometry and thus uncritically suggesting that the deformation during a orogenic scale happens periodically should be avoided (Park, 1969; Williams et al., 2008; Fossen and Cavalcante, 2017). Even structures which supposedly show perpendicular to orthogonal change in contraction could be explained by progressive and polyphase deformation (Fossen and Cavalcante, 2017).

This thesis has opted to use terms as deformation phases, D1-,D2- and so on, based mainly on geometry, orientation and overprinting relationships. This study cannot directly provide evidence for determining whether the described structures were formed during a progressive or polyphase deformation. Even so, a short summary of the main differences between phases are shown below for future work and interpretation.

D1-D2 The metamorphic conditions during D1 have been identified to upper- to middle amphibolite facies, while greenschist facies metamorphic conditions prevailed during the D2 phase (Pharaoh, 1981; Braathen, 1991; Andreassen, 1993; Davidsen, 1994; Braathen and Davidsen, 2000; Davidsen, 1994). Structures interpreted to form during the D1 phase display geometry and orientation which suggest W (Braathen and Davidsen, 2000) and NW directed shortening (this thesis), while the D2 shows a generally SW directed orogen parallel contraction.

D2-D3 The D2 and D3 structures were formed during greenschist metamorphic conditions (Pharaoh, 1981; Braathen, 1991; Andreassen, 1993; Davidsen, 1994; Braathen and Davidsen, 2000; Davidsen, 1994). Localized oblique shearing along the steep limbs of F2 appear to produce folds which are categorized as F3 folds which refold macro-scale F2 folds.

3.3 Tectonic model

Based on the structural data and the discussion above, a general structural model is proposed for the northern parts of the Lakselv area in the northern KGB (Fig.3.7).

The D1 phase is characterized by SE- and SW- dipping, penetrative foliation with accompanied SW-plunging stretching lineation. Several macro-scale isoclinal

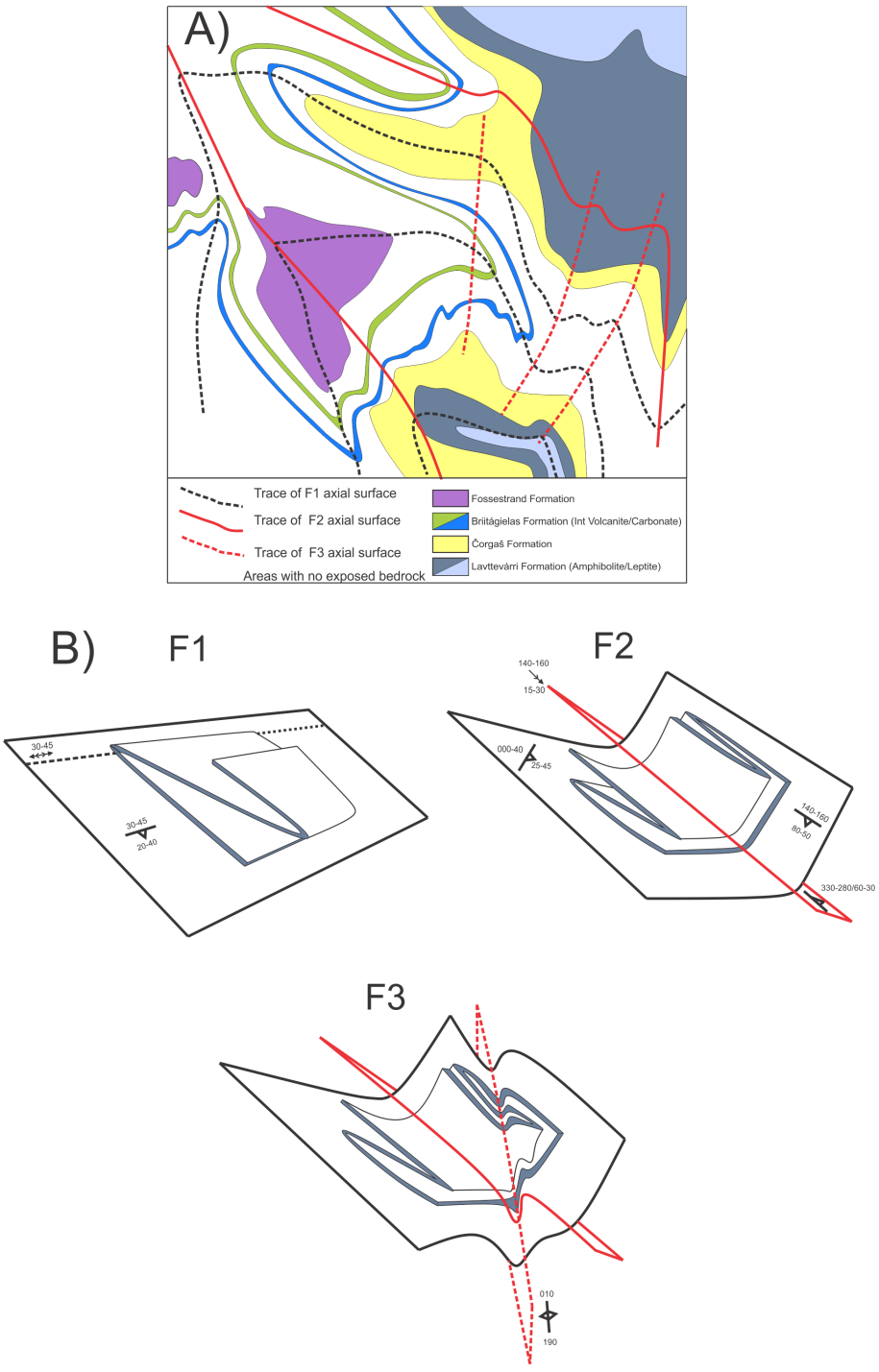

Figure 3.7: Combined tectonic model, shown as map view (A) and 3D-sketch interpretations (B) for the evolution of observed structures in the study area. A) Macro scale fold interference pattern in the study area showing F1-F2 patterns and related traces of F1-, F2-, and F3-, axial surfaces. B) 3D-sketch interpretation of evolution of planar structures (S1,S2,S3) as foliations and ductile shear zones formed axial-planar to the major F1-, F2-, and F3-folds in the study area. Note tight isoclinal F1-folds with S1-foliation, which are refolded perpendicular by a F2-assymetric, upright fold, and a set of apperent, conjugate, steeply-plunging F3-folds.

F1-folds which are strongly refolded by F2, indicate that the initial orientation and geometry before refolding was NW-vergent isoclinal moderately to gently inclined.

The D2 phase produced macro-scale asymmetric folds with SW-vergence and fold axes sub-parallel with the D1 stretching lineations. The refolding produced nearly vertical SW dipping F1 axial planes in the forelimb (study area) and gently E dipping F1 axial planes in the backlimb (west of study area). In the core, a refolding structure produced a typical Ramsey type 2 interference pattern.

The D3 phase is more local and display different geometries based on the initial strike and dip of the S1 foliation. In the steep F2 forelimbs, steeply plunging F3 shear folds with N-S striking axial planes, while in the gently SW dipping S1 foliation in the F2 backlimb, buckle folds are more common.

3.4 Regional implications and correlation

3.4.1 The Karasjok Greenstone Belt

The proposed new structural model for the northern part of the KGB (Fig.3.7) corresponds well with the established tectonic model for the whole KGB (Fig.1.7). The most noticeable difference is the D1 phase, which is interpreted to be the result of NW directed dip-slip, thrust related deformation and consequently NW vergent isoclinal F1-folds. The established model and interpretation of the Lakselv area based on the work of Pharaoh (1981); Andreassen (1993); Davidsen (1994) suggests that the D1 phase is characterized by a penetrative east-dipping foliation. This suggests a W-directed thrusting and refolding of the entire belt by an isoclinal recumbent fold with the Tanaelv Migmatite belt as the upper fold-limb roof (Braathen and Davidsen, 2000). However, Andreassen (1993) observed indications of W, SW and S directed movement in D1 shear zones, and suggests that later deformation did strongly affect the D1 structures. If the newly proposed model is plausible and not a local phenomenon, the implications could be substantial. This would suggest that the thrusting of the Tanaelv migmatite would more likely be related to the D2 phase in the KGB.

Geophysical data, Skaar (2014); Nasuti et al. (2015) show that there is a distinct difference in the orientation of lineaments in the north and the south of the KGB. In the north, the lineaments mostly strike NNW-SSW and E-W in the south. I addition, the Lakselv area show no distinct orienations for the lineaments. However, based on the general appearence, the Lakselv area displays more similarities with the southern parts of the KGB (Fig.3.8). The lineaments in the northern parts

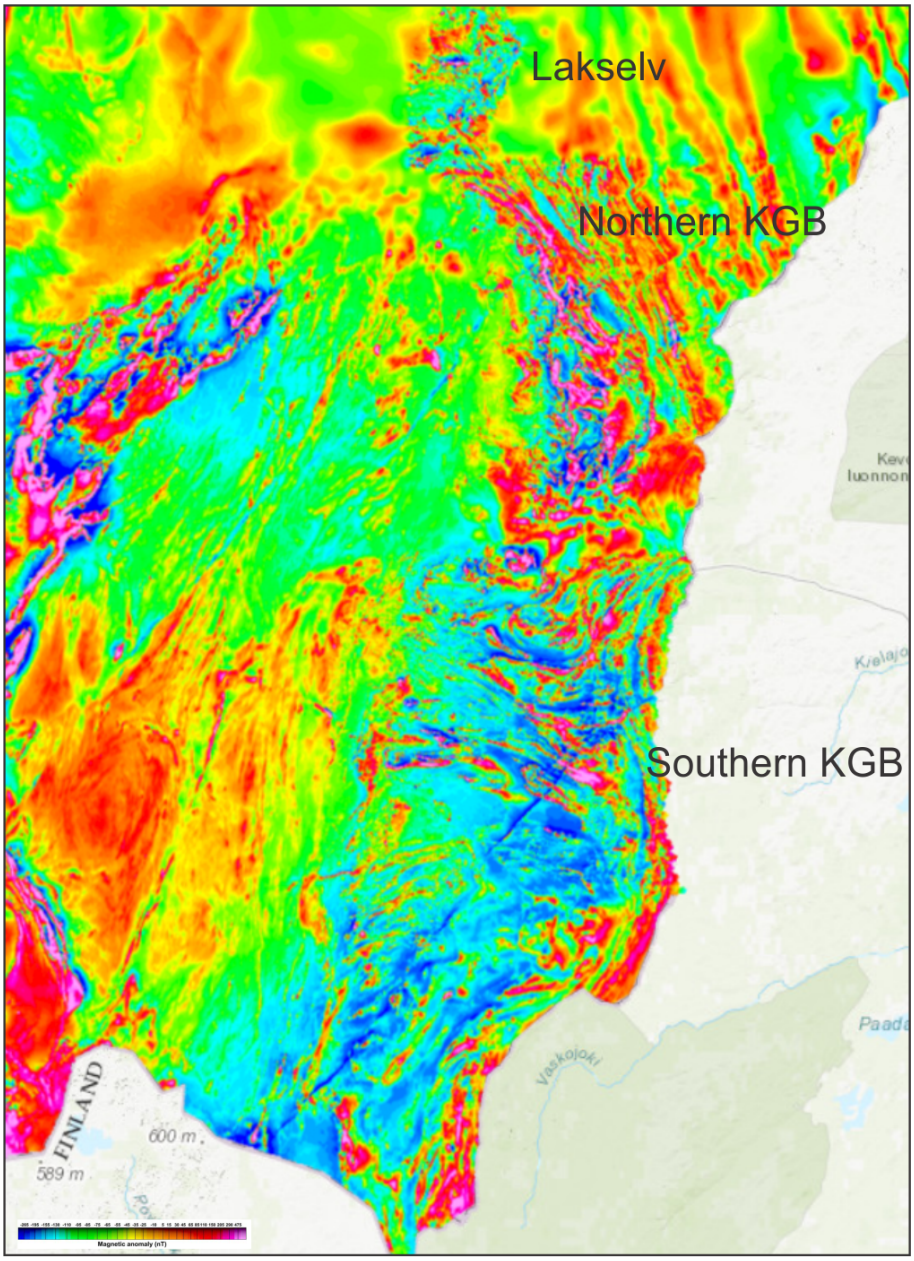

Figure 3.8: Magnetic data retrieved from www.NGU.no. Distinct orientation of lineaments categorzied as Lakselv, northern and southern based on the interpretation of (Nasuti et al., 2015).

correspond with the orientation of D2 structures in the Lakselv area. While the less distinct lineaments in the southern area could correspond to refolding structures seen in Lakselv. Note that although the northern parts seem fairly linear, geophysical modelling of the area suggests that refolding and gradually more complex structures are present towards the east in the KGB.

The D2 and D3 structures observed in the Lakselv area are consistent with the observed D2 and D3 structures seen elsewhere in the KGB.

3.4.2 Northeastern Fennoscandia

Recent structural and kinematic analysis of the Kautokeino Greenstone Belt, show that the belt can be divided into two tectonic compartments (Henderson et al., 2016). The NE-domain situated relatively close to the Lakselv area, displays pervasive NE-SW-trending anomalies, which have previously been described and interpreted to be structures related to the Mierujávri-Sværholt Fault Zone (Olesen and Sandstad, 1993). Structural data show that the foliation within the NE-domain generally strikes NE-SW and dips at very gentle to moderately to the NW or SE (Note axial planar parallel with the proposed F1 folds at Lakselv). These structures are also interpreted to be the earliest formed ductile structures in the NE parts of the Kautokeino Greenstone Belt (Henderson et al., 2016).

Further north, in the Repparfjord tectonic windows, a macro-scale upright NE-SW trending anticline affect the geometry of the area interpreted to be formed during the Svecofennian orogeny (c.1900-1750 Ma) (Torgersen et al., 2015; Bingen et al., 2016). The macro-scale fold in the Repparfjord Tectonic Window shows strike parallel axial planes with regards to the F1 folds interpreted in the Lakselv area. However, the geometry is different. Based on the youngest depositional age in the KGB (1950 Ma), one may reason for temporal correlation.

The West Troms Basement Complex also displays structures related to orogen perpendicular shortening (Bergh et al., 2007, 2010), mostly in the northern parts on the island of Vanna during the later part of the Svecofennian orogen, although recent geochronological data suggest post Caledonian ages, it is interpreted to be re-activation of Palaeoproterozoic SE directed thrusts (Paulsen et al., 2020).

The new D1 also suggests thrusting perpendicular to the orogen-normal during the early stages of the Lapland-Kola orogen which have been observed in the Inari orocline (Lapland granulite belt), although related to a younger deformational D3 phase (Lahtinen and Huhma, 2019). The KGB is interpreted to be a par-autochthonous unit (Braathen, 1991; Davidsen, 1994) in relationship with the Jergul-gneiss complex and a retro-arc basin related to the Lapland-Kola orogeny (Lahtinen and Huhma, 2019). Hence the D1 phase in the KGB could correspond

with later phases in the Lapland-Kola orogeny where contraction leads to the buckling and the arcute shape of the Lapland Granulite Belt Lahtinen et al. (2016). Simultaneously, the underlying KGB produced dip-slip thrusts and folds in parallel with the shape of the Inari orocline, thus leading to NW verging F1 folds in the northernmost part (Lakselv) and W verging thrusting and folding in the northern part, and finally SW verging folds and thrusting in the southern parts.

Several Archean gneiss-greenstone terranes exhibit dome and basin structures, suggesting that isostasi due to erosion was the first-order factor for orogenic events (Gapais et al., 2009; Cagnard et al., 2011). Younger gneiss-greenstone terranes exhibit modern-type tectonics with exhumed high /ultra-high pressure and low temperature rocks, accretion of units with a clear contrasting metamorphic grade and strain localisation along lithospheric-scale thrusts (Chardon et al., 2009). A combination of "Archean-type" and "modern-type" tectonics have been suggested for the Lapland-Kola orogen by Cagnard et al. (2011). Other authors, such as Lahtinen and Huhma (2019), suggest a modern type tectonic model for the same orogen. Nevertheless, the debate on the initiation of plate-tectonics is still a highly controversial topic (Bedard et al., 2003; Bedard, 2006; Maurice et al., 2009; Hamilton, 2011). Thus, a simple two endmember classification should probably be avoided(Stern, 2005; Hamilton, 2011; Gerya, 2014). Recognizing that a shift from hot Archean to colder modern-type tectonics could be spatially and temporal dependant (Van Kranendonk et al., 2004), and that a shift does not necessary exclude one process if evidence of another process is present, the different orientation of the D1 could be explained by this combination of tectonic styles as well as local differences and orogenic scale differences in strain could be an explanation for the apparent spatial changes in the D1 phase.

The Tanaelv Migmatite Belt and the Levajok Granulite Complex are previously interpreted to have been thrusted on top of the KGB during D1 (Krill et al., 1985; Marker, 1985; Braathen and Davidsen, 2000). The E to NE dipping thrusts seen at the boundary between KGB and The Tanaelv Migmatite Belt are sub-parallel with F2 axial planes and small-scale shear zones in the Lakselv area. This could be interpreted to be D2 structures. However, the Tanaelv Migmatite Belt is not exposed in the Lakselv area, a correlation is difficult to demonstrate.

Chapter 4

Conclusion

The main objectives of this study have been to perform a detailed structural analysis of the macro- to mesoscale folds found in the well exposed northern parts of the KGB. Further, less exposed areas in southern KGB will be compared with structures identified in in the field study area. In addition, localized overturned and out-of-sequence formations will be explained by obtained structural data.

A new structural model for the northern KGB, combined with a regional correlation, is summarized below:.

D1 — NW-directed thrusting and or imbrication produced SE dipping penetrative foliation and isoclinal to tight folds with axial planes dipping to the SE. F1 folds inverted the belt numerous places. Repetition of the stratigraphy can also be seen in the SW of the study area. The maximum age of the D1 phase is c.1950 Ma, which is the age of the youngest formation in northern KGB. The D1 can be structurally correlated with the northeastern part of the Kautokeino Greenstone Belt and the Jergul Gneiss Complex and could be the result of a distant Svecofennian contraction.

D2 — Highly asymmetric macro and mesoscale F2 folds refolded the preexisting F1 structures and thus created macro scale interference patterns. The F2 folds verge to the SW with steep to moderate dipping axial planes. The D2 structures correlate well with the large thrust seen at the base of the Tanaelv Migmatite Belt. This phase is therefore related to the Lapland-Kola orogeny.

D3 — Localized shearing along the existing steep limbs of F1 and F2 produced kink like fault propagation folds with N-S trending near vertical axial planes. They refold both D1 and D2 structures. The D3 phase is the result of progressive, steady state deformation. D3 could possible be categorized as a late D2 structure.

Further work — would include the testing of the structural model for other areas. First in other parts of the Lakselv area, and later throughout the KGB. An effort of dating the different structures would help understand the Svecofennian and the Lapland-Kola evolution in time and place and thus the tectonic history of the northwestern parts of the Fennoscandian shield.

References

Allmendinger, R.W., 1998. Inverse and forward numerical modeling of trishear fault-propagation folds. Tectonics 17, 640–656. doi:Doi10.1029/98tc01907.

Andreassen, T.O., 1993. Strukturelle of tektoniske undersøkelser i de nordlige deler av Karasjok grønnsteinsbelte, Finnmark fylke. Cand. scient. thesis. University of Tromsø.

Bedard, J.H., 2006. A catalytic delamination-driven model for coupled genesis of archaean crust and sub-continental lithospheric mantle. Geochimica Et Cosmochimica Acta 70, 1188–1214. doi:10.1016/j.gca.2005.11.008.

Bedard, J.H., Brouillette, P., Madore, L., Berclaz, A., 2003. Archaean cratonization and deformation in the northern superior province, canada: an evaluation of plate tectonic versus vertical tectonic models. Precambrian Research 127, 61–87. doi:10.1016/S0301-9268(03)00181-5.

Bergh, S., Corfu, F., Priyatkina, N., Kullerud, K., Myhre, P., 2015. Multiple post-Svecofennian 1750–1560 Ma pegmatite dykes in Archaean-Palaeoproterozoic rocks of the West Troms Basement Complex, North Norway: Geological significance and regional implications. Precambrian Research 266, 425 – 439. doi:https://doi.org/10.1016/j.precamres.2015.05.035.

Bergh, S.G., Kullerud, K., Armitage, P.E., Zwaan, K.B., Corfu, F., Ravna, E.J., Myhre, P.I., 2010. Neoarchaean to Svecofennian tectono-magmatic evolution of the West Troms Basement Complex, North Norway. Norwegian Journal of Geology 90, 21–48.

Bergh, S.G., Kullerud, K., Corfu, F., Armitage, P.E., Davidsen, B., Johansen, H.W., Pettersen, T., Knudsen, S., 2007. Low-grade sedimentary rocks on Vanna, North Norway: a new occurrence of a Palaeoproterozoic (2.4-2.2 Ga) cover succession in northern Fennoscandia. Norwegian Journal of Geology 87, 301–318.

Bergmann, S., 2018. Geology of Northern Norrbotten ore province, northern Sweden. techreport 141. Geological Survey of Sweden.

Bingen, B., Solli, A., Viola, G., Torgersen, E., Sandstad, J.S., Whitehouse, M.J., Røhr, T.S., Ganerød, M., Nasuti, A., 2016. Geochronology of the palaeoproterozoic kautokeino greenstone belt, finnmark, norway: Tectonic implications in a fennoscandia context. Norwegian Journal of Geology doi:10.17850/njg95-3-09.

Braathen, A., 1991. Stratigrafi og strukturgeologi sentralt i Karasjok grønnsteinsbelte, Finnmark. Cand. scient. thesis. University of Tromsø.

Braathen, A., Davidsen, B., 2000. Structure and stratigraphy of the Palaeoproterozoic Karasjok Greenstone Belt, north Norway - regional implications. Norsk Geologisk Tidsskrift 80, 33–50.

Burg, J.P., Podladchikov, Y., 2000. From buckling to asymmetric folding of the continental lithosphere: numerical modelling and application to the himalayan syntaxes. Geological Society, London, Special Publications 170, 219–236. doi:10.1144/GSL.SP.2000.170.01.12.

Cagnard, F., Barbey, P., Gapais, D., 2011. Transition between "Archaean-type" and "modern-type" tectonics: Insights from the Finnish Lapland Granulite Belt. Precambrian Research 187, 127–142. doi:10.1016/j.precamres.2011.02.007.

Carreras, J., Cosgrove, J.W., Druguet, E., 2013. Strain partitioning in banded and/or anisotropic rocks: Implications for inferring tectonic regimes. Journal of Structural Geology 50, 7 – 21. doi:https://doi.org/10.1016/j.jsg.2012.12.003. deformation localization in rocks.

Carreras, J., Druguet, E., 2019. Complex fold patterns developed by progressive deformation. Journal of Structural Geology 125, 195–201. doi:10.1016/j.jsg.2018.07.015.

Chardon, D., Gapais, D., Cagnard, F., 2009. Flow of ultra-hot orogens: A view from the precambrian, clues for the phanerozoic. Tectonophysics 477, 105–118. doi:10.1016/j.tecto.2009.03.008.

Corfu, F., Hanchar, J.M., Hoskin, P.W., Kinny, P., 2003. Atlas of zircon textures. Reviews in Mineralogy and Geochemistry 53, 469–500. doi:10.2113/0530469.

Dahlstrom, C.D., 1970. Structural geology in eastern margin of canadian rocky-mountains. American Association of Petroleum Geologists Bulletin 54, 843–+. URL: <GotoISI>://WOS:A1970G378400040.

Davidsen, B., 1994. Stratigrafi, petrologi og geokjemi med vekt på komatiittiske bergarter innen den nordligste del av Karasjok grønnsteinsbelte, Brennelv, Finnmark. Cand. scient. thesis. University of Tromsø.

Eilu, P., 2017. Fennoscandian orogenic gold in the context of regional orogenic evolution. Mineral Resources to Discover, Vols 1-4 , 23–26.

Eilu, P., Ojala, V.J., 2011. Cu-au mineralisation at raitevarri, karasjok greenstone belt, northern norway. Let's Talk Ore Deposits, Vols I and Ii , 350–352.

Eilu, P., Sorjonen-Ward, P., Nurmi, P., Niiranen, T., 2003. A review of gold mineralization styles in finland. Economic Geology and the Bulletin of the Society of Economic Geologists 98, 1329–1353. doi:Doi10.2113/98.7.1329.

Erslev, E.A., 1991. Trishear fault-propagation folding. Geology 19, 617–620. doi:Doi10.1130/0091-7613(1991)019<0617:Tfpf>2.3.Co;2.

Fossen, H., Cavalcante, G.C.G., 2017. Shear zones - a review. Earth-Science Reviews 171, 434–455. doi:10.1016/j.earscirev.2017.05.002.

Gaál, G., Gorbatschev, R., 1987. An outline of the precambrian evolution of the baltic shield. Precambrian Research 35, 15–52. doi:10.1016/0301-9268(87)90044-1.

Gapais, D., Cagnard, F., Gueydan, F., Barbey, P., Ballevre, M., 2009. Mountain building and exhumation processes through time: inferences from nature and models. Terra Nova 21, 188–194. doi:10.1111/j.1365-3121.2009.00873.x.

Gerya, T., 2014. Precambrian geodynamics: Concepts and models. Gondwana Research 25, 442–463. doi:10.1016/j.gr.2012.11.008.

Gorbatschev, R., Bogdanova, S., 1993. Frontiers in the Baltic Shield. Precambrian Research 64, 3–21.

Grasemann, B., Wiesmayr, G., Draganits, E., Fusseis, F., 2004. Classification of refold structures. The Journal of Geology 112, 119–125. doi:10.1086/379696.

Groves, D.I., Santosh, M., Goldfarb, R.J., Zhang, L., 2018. Structural geometry of orogenic gold deposits: Implications for exploration of world-class and giant deposits. Geoscience Frontiers 9, 1163–1177. doi:10.1016/j.gsf.2018.01.006.

Hamilton, W.B., 2011. Plate tectonics began in neoproterozoic time, and plumes from deep mantle have never operated. Lithos 123, 1–20. doi:10.1016/j.lithos.2010.12.007.

Hansen, H., Slagstad, T., Bergh, S.G., 2020. Geochemical volcanostratigrapy defines the tectonic evolution of the karasjok greenstone belt, finmark doi:10.13140/RG.2.2.34380.16001.

Hanski, E., Huhma, H., Vaasjoki, M., 2001. Geochronology of northern Finland: a summary and discussion, in: Vaasjoki, M. (Ed.), Radiometric age determinations from Finnish Lapland and their bearing on the timing of Precambrian volcano-sedimentary sequences. Geological Survey of Finland. volume 33 of *Special Paper*, pp. 255–279. URL: http://tupa.gtk.fi/julkaisu/specialpaper/sp_033.pdf. 8 Figures and one table.

Henderson, I.H., Viola, G., Nasuti, A., 2016. A new tectonic model for the palaeoproterozoic kautokeino greenstone belt, northern norway, based on high-resolution airborne magnetic data and field structural analysis and implications for mineral potential. Norwegian Journal of Geology doi:10.17850/njg95-3-05.

Humair, F., Bauville, A., Epard, J.L., Schmalholz, S.M., 2020. Interaction of folding and thrusting during fold-and-thrust-belt evolution: Insights from numerical simulations and application to the swiss jura and canadian foothills. Tectonophysics , 228474doi:https://doi.org/10.1016/j.tecto.2020.228474.

Jamison, W.R., 1987. Geometric analysis of fold development in overthrust terranes. Journal of Structural Geology 9, 207–219. doi:Doi10.1016/0191-8141(87)90026-5.

Jordan, T.E., Allmendinger, R.W., 1986. The sierras pampeanas of argentina - a modern analog of rocky-mountain foreland deformation. American Journal of Science 286, 737–764. doi:DOI10.2475/ajs.286.10.737.

Karki, A., Laajoki, K., Luukas, J., 1993. Major palaeoproterozoic shear zones of the central fennoscandian shield. Precambrian Research 64, 207–223. doi:Doi10.1016/0301-9268(93)90077-F.

Krabbendam, M., Leslie, A., 1996. Folds with vergence opposite to the sense of shear. Journal of Structural Geology 18, 777 – 781. doi:https://doi.org/10.1016/S0191-8141(96)80011-3.

Krill, A., Bergh, S., Lindahl, I., Mearns, E., Often, M., Olerud, S., Olesen, O., Sandstad, J., Siedlecka, A., Solli, A., 1985. Rb-Sr, U-Pb and Sm-Nd isotopic dates from Precambrian rocks of Finnmark. Norges geologiske undersøkelse Bulletin 403, 37–54.

Krill, A.G., 1985. Svekokarelian thrusting with thermal inversion in the Karasjok-Levajok area of the northern Baltic Shield. Norges geologiske undersøkelse Bulletin 403, 89–101.

Lahtinen, R., Garde, A.A., Melezhik, V.A., 2008. Paleoproterozoic evolution of Fennoscandia and Greenland. Episodes 31, 20–28.

Lahtinen, R., Huhma, H., 2019. A revised geodynamic model for the lapland-kola orogen. Precambrian Research 330, 1–19. doi:10.1016/j.precamres.2019.04.022.

Lahtinen, R., Huhma, H., Lahaye, Y., Lode, S., Heinonen, S., Sayab, M., Whitehouse, M.J., 2016. Paleoproterozoic magmatism across the Archean-Proterozoic boundary in central Fennoscandia: Geochronology, geochemistry and isotopic data (Sm–Nd, Lu–Hf, O). Lithos 262, 507–525. doi:https://doi.org/10.1016/j.lithos.2016.07.014.

Lahtinen, R., Korja, A., Nironen, M., 2005. Paleoproterozoic tectonic evolution, in: Lehtinen, M., Nurmi, P., Rämö, O. (Eds.), Precambrian Geology of Finland — Key to the Evolution of the Fennoscandian Shield. Elsevier. volume 14 of *Developments in Precambrian Geology*. chapter 11, pp. 481–531. doi:10.1016/s0166-2635(05)80012-x.

Marker, M., 1985. Early proterozoic (c. 2000-1900 ma) crustal strucutre of the northeastern baltic shield: tectonic division and tectogenesis. Norges geologiske undersøkelse Bulletin 403, 55–74.

Marker, M., Kaulina, T., Daly, J., 2000. New evidence for the Proterozoic evolution of the Tanaelv and Karasjok belts based on Sm-Nd data and recent U-Pb NORDSIM and TIMS dating from Finnmark, Norway. techreport 23. University of Oulu.

Maurice, C., David, J., Bedard, J.H., Francis, D., 2009. Evidence for a widespread mafic cover sequence and its implications for continental growth in the northeastern superior province. Precambrian Research 168, 45–65. doi:10.1016/j.precamres.2008.04.010.

Melezhik, V.A., Hanski, E.J., 2013. Palaeotectonic and Palaeogeographic Evolution of Fennoscandia in the Early Palaeoproterozoic, in: Melezhik, V.A., Prave, A.R., Hanski, E.J., Fallick, A.E., Lepland, A., Kump, L.R., Strauss, H. (Eds.), Reading the Archive of Earth's Oxygenation. Springer. Frontiers in Earth Sciences. chapter 3.3, pp. 111–178. doi:10.1007/978-3-642-29682-6_5.

Melezhik, V.A., Solli, A., Fallick, A.E., Davidsen, B., 2015. Chemostratigraphic constraints on the time of deposition of carbonate rocks in the Karasjok Greenstone Belt, northern Norway. Norwegian Journal of Geology 95, 299–314. doi:http://dx.doi.org/10.17850/njg95-3-03.

Mukherjee, S., 2017. Review on symmetric structures in ductile shear zones. International Journal of Earth Sciences 106, 1453–1468. doi:10.1007/s00531-016-1366-4.

Myhre, P.I., Corfu, F., Bergh, S.G., 2011. Palaeoproterozoic (2.0–1.95 Ga) pre-orogenic supracrustal sequences in the West Troms Basement Complex, North Norway. Precambrian Research 186, 89–100. doi:10.1016/j.precamres.2011.01.003.

Myhre, P.I., Corfu, F., Bergh, S.G., Kullerud, K., 2013. U–Pb geochronology along an Archaean geotransect in the West Troms Basement Complex, North Norway. Norwegian Journal of Geology 93, 1–24.

Nasuti, A., Roberts, D., Dumais, M.A., Ofstad, F., Hyvönen, E., Stampolidis, A., 2015. New high-resolution aeromagnetic and radiometric surveys in Finnmark nad North Troms: linking anomaly patterns to bedrock geology and structure. Norwegian Journal of Geology 95, 217–244.

Nilsen, K., 1988. Beskrivelse til det berggrunnsgeologiske kart Karasjok 2033 I, M 1:50.000. techreport 88.208. NGU.

Nilsen, K., 1989. Stratigraphic and structural geology of south and west of Porsangermoen, Lakselv valley, northern Norway. techreport. NGU.

Often, M., 1985. The Early Proterozoic Karasjok Greenstone Belt, Norway: a preliminary description of lithology, stratigraphy and mineralization. Norges geologiske undersøkelse Bulletin 403, 75–88.

Olesen, O., Sandstad, J., 1993. Interpretation of the Proterozoic Kautokeino Greenstone Belt, Finnmark, Norway. Norges geologiske undersøkelse Bulletin 425, 43–67.

Park, R., 1969. Structural correlation in metamorphic belts. Tectonophysics 7, 323 – 338. URL: http://www.sciencedirect.com/science/article/pii/0040195169900778, doi:https://doi.org/10.1016/0040-1951(69)90077-8.

Paulsen, H.K., Bergh, S.G., Palinkas, S.S., 2020. Late Palaeozoic fault-controlled hydrothermal cu-zn mineralisation on Vanna island, West Troms Basement Complex, northern Norway. Norwegian Journal of Geology , 1–41doi:10.17850/njg100-1-2.

Pharaoh, T., 1981. Preliminary report on the geology of the northern part of the Lakselv valley,Finnmark, Northern Norway. techreport 016-81. NGU.

Poblet, J., Lisle, R.J., 2011. Kinematic evolution and structural styles of fold-and-thrust belts. Geological Society, London, Special Publications 349, 1–24. doi:10.1144/SP349.1.

Ramsey, J., 1962. Interference patterns produced by the superposition of folds of "similar" type. Journal of Geology 60, 466–481.

Saalmann, K., Laine, E.L., 2014. Structure of the outokumpu ore district and ophiolite-hosted cu-co-zn-ni-ag-au sulfide deposits revealed from 3d modeling and 2d high-resolution seismic reflection data. Ore Geology Reviews 62, 156–180. doi:10.1016/j.oregeorev.2014.03.003.

Saalmann, K., Mänttäri, I., Peltonen, P., Whitehouse, M.J., Grönholm, P., Talikka, M., 2010. Geochronology and structural relationships of mesothermal gold mineralization in the Palaeoproterozoic Jokisivu prospect, southern Finland. Geological Magazine 147, 551–569. doi:10.1017/s0016756809990628.

Saalmann, K., Niiranen, T., 2010. Hydrothermal alteration and structural control of gold deposition in the Hanhimaa shear zone and western part of the Sirkka Line. techreport M19/2741/2010/58. GTK.

Sandstad, J.S., 2015. MINN - Mineral resources in North Norway. Norwegian Journal of Geology 95, 211–216.

Siedlecka, A., Iversen, E., Krill, A.G., Lieungh, B., Often, M., Sandstad, J.S., Solli, A., 1985. Lithostratigraphy and correlation of the Archean and Early Proterozoic rocks of Finnmarksvidda and the Sørvaranger district. Norges geologiske undersøkelse Bulletin 403, 7–36.

Skaar, J., 2014. 3D geophysical and geological modelling of the Karasjok Greenstone Belt. Msc thesis. Norwegian University of Science and Technology.

Stern, R.J., 2005. Evidence from ophiolites, blueschists, and ultrahigh-pressure metamorphic terranes that the modern episode of subduction tectonics began in neoproterozoic time. Geology 33, 557–560. doi:10.1130/G21365.1.

Thiessen, R.L., Means, W.D., 1980. Classification of fold interference patterns - a reexamination. Journal of Structural Geology 2, 311–316. doi:Doi10.1016/0191-8141(80)90019-X.

Torgersen, E., Viola, G., Sandstad, J.S., 2015. Revised structure and stratigraphy of the northwestern Repparfjord Tectonic Window, northern Norway. Norwegian Journal of Geology 95, 397–421. doi:10.17850/njg95-3-06.

Van Kranendonk, M.J., Collins, W.J., Hickman, A., Pawley, M.J., 2004. Critical tests of vertical vs. horizontal tectonic models for the archaean east pilbara granite-greenstone terrane, pilbara craton, western australia. Precambrian Research 131, 173–211. doi:DOI10.1016/j.precamres.2003.12.015.

Williams, I.S., Rutland, R.R., Kousa, J., 2008. A regional 1.92 Ga tectonothermal episode in Ostrobothnia, Finland: Implications for models of Svecofennian accretion. Precambrian Research 165, 15–36. doi:10.1016/j.precamres.2008.05.004.

Zhang, Q., Fossen, H., 2020. The dilemma of asymmetric porphyroclast systems and sense of shear. Journal of Structural Geology 130. doi:ARTN10389310.1016/j.jsg.2019.103893.